https://doi.org/10.5194/egusphere-2026-4201
Preprint. Discussion started: 27 July 2026

Storage and connectivity across river corridor and watershed scales in three headwater streams of the southeastern USA

Delaney M. Peterson[1,2], C. Nathan Jones[1], Stephen Plont[3,1], Sarah E. Godsey[4], Kaci Zarek[5], Adam S. Ward[2], Carla L. Atkinson[1]

[1]Department of Biological Sciences, University of Alabama, Tuscaloosa AL, 35487, USA
[2]Department of Biological and Ecological Engineering, Oregon State University, Corvallis OR, 97331, USA
[3]Odum School of Ecology, University of Georgia, Athens GA, 30602, USA
[4]Department of Geosciences, Idaho State University, Pocatello ID, 83209, USA
[5]Department of Ecology and Evolutionary Biology, Cornell University, Ithaca NY, 14850, USA

Correspondence to: Delaney M. Peterson (dmpeterson2@crimson.ua.edu)

Abstract. Watershed characteristics create a mosaic of potential storage zones, and linkages between these result in hydrologic connectivity between groundwaters and surface waters. Watershed storage and connectivity are fundamental controls on stream network dynamics, yet predicting the patterns of hydrologic responses like streamflow remains difficult due to landscape heterogeneity across multiple, interacting spatial scales. Here, we characterize storage and connectivity dynamics at the watershed scale and the hydrogeomorphic feature (HGF) scale using a network of steam and riparian groundwater monitoring wells in three watersheds spanning the Coastal Plain, Piedmont, and Appalachian Plateaus physiographic regions of the southeastern USA. At the watershed scale, we operationalized watershed storage as the slope of streamflow recession at the watershed outlet, and hydrologic connectivity as the relationship between outlet discharge and network length. At the HGF scale, we operationalized storage as the slope of water level recession at seven in-stream monitoring locations, and connectivity as the lateral hydraulic gradient and water level hysteresis relationships between the stream channel and adjacent riparian zone at three locations per watershed. At the watershed scale, we found patterns in storage and connectivity varied across physiographic regions. We also found distinct storage and connectivity dynamics across HGFs, many of which challenged existing conceptualizations for similar geomorphic settings. Notably, channel incision emerged as a key structural control, homogenizing storage and connectivity patterns across otherwise disparate watersheds and producing a common threshold response in watershed storage. Together, these results demonstrate that watershed-scale patterns do not reflect the heterogeneity observed at the HGF scale. Moreover, river corridor structure, particularly channel incision, is a key driver of storage and connectivity dynamics across physiographic settings.

1 Introduction

Stream networks integrate watershed heterogeneity and climatic variability, generating dynamic streamflow responses and challenging our ability to parse individual drivers of these processes. Streams are dynamic landscape features whose hydrologic conditions vary across both space and time (Godsey & Kirchner, 2014; Durighetto & Botter, 2022). It is

https://doi.org/10.5194/egusphere-2026-4201
Preprint. Discussion started: 27 July 2026

well understood that conditions in and around the stream channel are a function of valley characteristics (e.g., Hynes, 1975; Larkin and Sharp, 1992), and variability in responses like streamflow and network extent between watersheds is a function of climate, geology, vegetation, and land use (e.g., Costigan et al., 2016; Prancevic & Kirchner, 2019; Ward et al., 2018; Zipper et al., 2021). Further, variability of streamflow and network extent in the same network across time is impacted by temporal variability in watershed characteristics (e.g., seasonality in evapotranspiration; Barnard et al., 2010; Newcomb & Godsey, 2023). However, many hydrologic responses are nonlinear, exhibit threshold behaviors, and have controls spanning spatiotemporal scales, all of which combine to yield observable patterns in streamflow and connectivity (Jencso et al., 2009; Tromp-van Meerveld & McDonnell, 2006b; Spence, 2010). Thus, our overarching goal in this study is to evaluate how watershed characteristics modulate storage and connectivity across scales to drive stream network dynamics.

Storage and connectivity are conceptualized as the overarching drivers of watershed hydrologic processes, yet these characteristics are difficult to quantify as they are influenced by both static and dynamic watershed variables. Specifically, storage is defined broadly as the volume of water retained within a watershed across various compartments (e.g., soil moisture, snowpack; McNamara et al., 2011; McDonnell et al., 2018). Many studies have attempted to quantify storage as the volume of permeable material that can hold and release water using subsurface imaging (e.g., Holbrook et al., 2014; Collins et al., 1989) or as the volume of valleys, riparian zones, lakes, or wetlands (e.g., Jones et al., 2018). However, it can be difficult to define the absolute volume of storage zones within watersheds. For example, identifying the exact transition to impermeable bedrock to characterize soil depth is challenging (Sayama et al., 2011). As a result, storage is often measured as the change in storage in a system, such as the active storage compared to potential or total storage (Pfister et al., 2017). To this end, many studies have used soil moisture as a proxy for the dynamic soil storage component (Peters & Aulenbach, 2011) or storage release via streamflow (e.g., mean transit time, streamflow recession slope; Hrachowitz et al., 2009; Harman et al., 2009). This dynamic storage approach provides an opportunity to characterize storage released using readily measurable watershed responses; in the case of recession analyses, streamflow is straightforward to quantify, and flashiness and the rate of streamflow response is related to the size and stability of the contributing storage zones (Clark et al., 2009; Harman et al., 2009). Previous studies have found that storage is generally controlled by physiographic characteristics like underlying lithology (Price, 2011; Onda et al., 2001), soil characteristics (McNamara et al., 2011), and topographic gradients (Sayama et al., 2011; McGuire et al., 2005), though the importance of individual drivers is complicated both by the scales of interest as well as spatial heterogeneity in these characteristics. While storage represents physical characteristics of the watershed, connectivity is the resulting fluxes between storage zones.

Hydrologic connectivity is defined as the water-mediated movement of materials, organisms, and energy through the landscape (Pringle et al., 2001; Jones et al., 2019). One way of operationalizing this definition is to assess fluxes of water, energy, and/or materials across multiple dimensions. For example, connectivity is often quantified across time in three primary dimensions: vertical as deep and shallow subsurface flowpath connection (e.g., Zimmer & McGlynn, 2018), lateral or horizontal as lateral exchange flows (e.g., Harvey & Gooseff, 2015), and longitudinal as discharge and runoff or as longitudinal network extent (e.g., Spence, 2010; Zimmer & McGlynn, 2018). Like storage, many studies have documented that physical

https://doi.org/10.5194/egusphere-2026-4201
Preprint. Discussion started: 27 July 2026

watershed characteristics can control connectivity; at the network scale, topographic variables like slope can control the extent and dynamics of the network (Prancevic & Kirchner, 2019), whereas at more localized scales, heterogeneities in soil structure and depth (Tromp-van Meerveld & McDonnell, 2006b; Menichino & Hester, 2015), topographic gradients (Jencso & McGlynn, 2011), and even channel incision (Chen et al., 2020) can introduce points of (dis)connectivity and regulate local hydraulic gradients. However, measures of connectivity are defined by the discrete storage zones that fluxes are being measured between, making it difficult to identify universal metrics that can be quantified within and across watersheds (Bracken et al., 2013). Moreover, when defining storage using dynamic approaches like streamflow recession (as streamflow is also inherently an indicator of connectivity) it can be difficult to differentiate storage from connectivity. Challenges differentiating storage and connectivity are compounded by the integrative nature of stream networks, where conditions at the outlet are influenced by interacting upstream and local drivers, yet outlets are the location where streamflow is most commonly measured. Therefore, we lack an understanding of how dynamics in both storage and connectivity, and their interactions, drive processes within and across hydrologic systems.

Many outlet-focused metrics of storage and connectivity fail to resolve heterogeneity within watersheds because of the inherent scaling and integrative nature of networks (Harman et al, 2009). Put plainly, the patterns observed at the outlet cannot be separated from the location chosen for observation. There have been many calls to investigate key watershed compartments and "functional units" in an attempt to understand within-watershed dynamics that are expressed at the outlet (e.g., McGlynn et al., 2004; Spence, 2010; McDonnell et al., 2007). Previous work in headwater systems has primarily investigated compartments spanning from individual hillslopes (e.g., Tromp-van Meerveld & McDonnell, 2006a) to stream reaches to networks (e.g., Allen et al., 2018). Additional studies have integrated across these compartments as well by characterizing connectivity from hillslopes to riparian zones to streams (Jencso et al., 2009) or by quantifying exchange flows across entire valley-bottoms (river corridors; Gooseff & Harvey, 2015). Hydrogeomorphic features (hereafter, HGFs) represent an intermediate spatial scale that have recently been used to address the gap between discrete hillslope units and stream reaches. HGFs are defined as a functional unit of the river corridor that incorporate stream channels, riparian zones, and adjacent hillslopes, and are delineated based on distinct geomorphic characteristics that are both formed by and contribute to hydrologic patterns (Peterson et al., 2025). HGFs have been used to investigate groundwater-surface water and network hydrologic connectivity in a low-relief headwater watershed (Peterson et al., 2025) as well as inundation dynamics across common geomorphic units in a lowland fifth-order river-floodplain system (Cain et al., 2025) Characterizing storage and connectivity within watersheds at the scale of HGFs provides a unique opportunity to quantify how distinct structural characteristics of the river corridor drive hydrologic responses, as well as how signals from discrete geomorphic features within the network cascade to watershed outlets.

Here, our overarching objective was to assess the degree to which storage and connectivity dynamics explain within- and between-watershed variability in the southeastern USA. Specifically, we sought (i) to characterize storage and connectivity dynamics at the watershed- and HGF-scale to evaluate variability across physiographic settings, (ii) to compare indicators of connectivity and storage dynamics between the watershed and HGF scales, and (iii) to identify structural features that produce

https://doi.org/10.5194/egusphere-2026-4201
Preprint. Discussion started: 27 July 2026

consistent storage and connectivity patterns across HGFs regardless of broader watershed context. Towards these goals, we intensively monitored watersheds in three distinct physiographic regions throughout the 2023 and 2024 water-years, measuring streamflow, surface water and groundwater levels, and network extent to quantify proxies for storage and connectivity at both the watershed and HGF scales.

2 Methods

2.1 Site Descriptions

We selected three study watersheds across the state of Alabama that spanned the natural physiographic gradient in the southeastern USA (Fig. 1a-b). All three watersheds share a humid subtropical climate and have relatively similar precipitation inputs (approximately 1,400 mm per year; NOAA NCEI, 2025). Each watershed was instrumented with a network of surface water and groundwater monitoring sensors that we used to quantify water level recession, stream channel gain or loss, water level hysteresis, and longitudinal network connectivity. For more information on these research watersheds and monitoring infrastructure, see Plont et al. (2026). All analyses were performed in R version v 4.4.0 (R Core Team, 2024).

The study watershed in the Appalachian Plateaus physiographic province drains 2.97 km^2 of an unnamed tributary of Burks Creek in Jackson County (AL; Fig. 1c). This watershed has the highest relief of the three watersheds, spanning from 211 to 550 m above sea level (hereafter, m.a.s.l.) with slopes up to 69% (Peterson et al., 2026). This watershed is underlain by primarily sedimentary, karstic lithologic units, and in the headwaters specifically, exposure of the Bangor limestone unit results in abundant cave-springs and discharges from fractures (Ponta, 2018). Steep slopes and geologic erosion have resulted in thin, stony slopes and little soil development in this watershed (Swenson, 1941), and stream channels in the headwaters are predominantly exposed bedrock that grades into more depositional zones near the watershed outlet (Peterson et al., 2026; Soil Survey Staff, 2025). This watershed is almost entirely forested by mixed-age deciduous species, with dominant vegetation types of mixed oaks, beech, yellow-poplar, maples, and river birch (Griffith et al., 2001).

The study watershed in the Piedmont physiographic province drains 0.92 km^2 of an unnamed tributary to Pendergrass Creek in Cleburne County (AL; Fig. 1d). This is a moderate relief watershed, with elevation spanning from 345 to 456 m.a.s.l. and slopes up to 49% (Peterson, et al., 2026). This watershed is underlain by low-grade metamorphic rocks that are heavily fractured (Kopaska-Merkel et al., 2000). The headwaters of the watershed have thin, rocky soils and coarse stream sediments that grade into highly weathered, argillic soils and a mix of coarse and fine stream sediments closer to the watershed outlet (Zarek et al., 2025; Feminella, 1996; Soil Survey Staff, 2025). This watershed is completely forested with mixed deciduous and coniferous species, with predominantly pines in higher elevation and upland areas and mixed oak species throughout (Griffith et al., 2001; Plont et al., 2026).

https://doi.org/10.5194/egusphere-2026-4201
Preprint. Discussion started: 27 July 2026

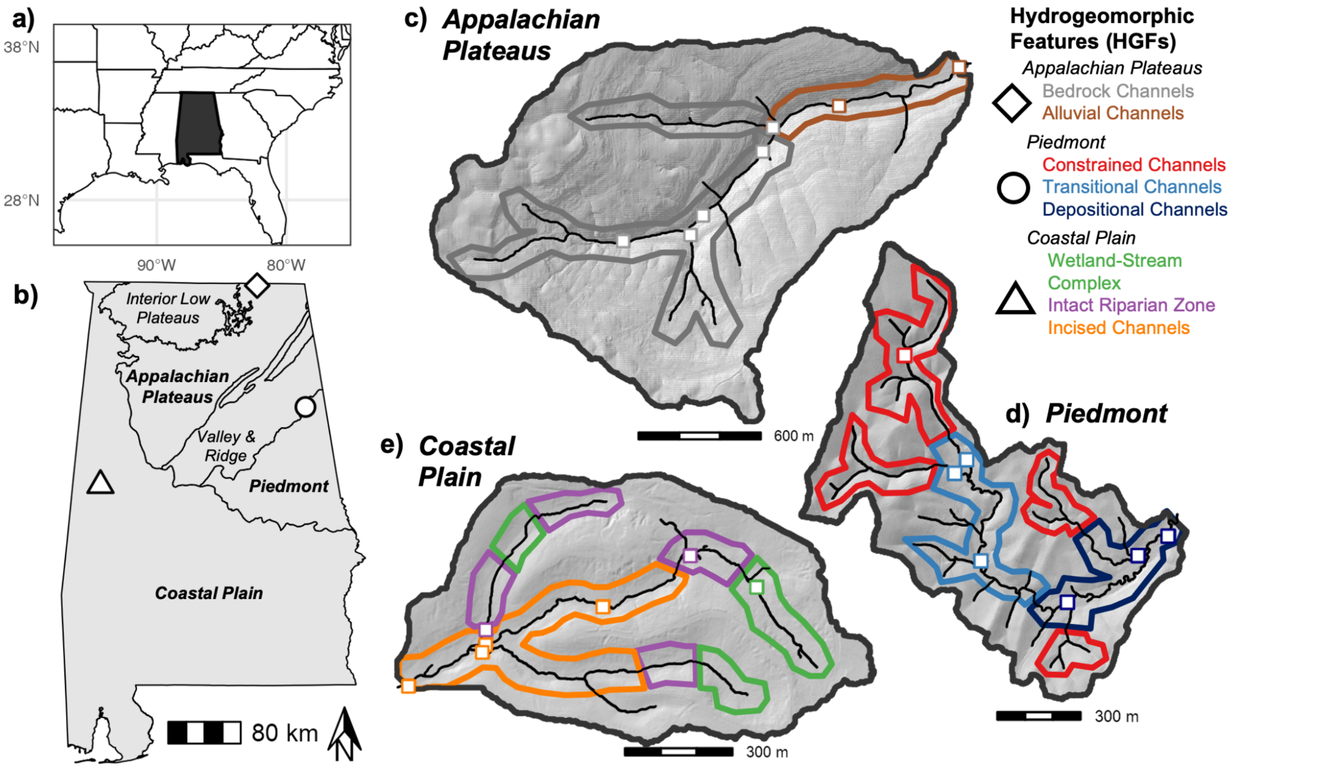

Figure 1: (a) A map of the southeastern USA, with the state of Alabama indicated in black for further context in (b). (b) A map of the physiographic regions of Alabama, where shapes indicate the three research watersheds in this study (c-e) and their respective regions noted by bold text. (c-e) A map of each research watershed, with the primary HGFs indicated by colored polygons, and the monitoring network indicated by squares on the stream network (black lines), also colored by HGF. Topography is indicated as hillshade. See legend for HGF colors.

Finally, the watershed in the Coastal Plain physiographic province drains 0.70 km^2 of an unnamed tributary of Shambley Creek in Greene County (AL; Fig. 1e). This watershed has the lowest relief of the three watersheds, spanning from 63 to 94 m.a.s.l. and slopes up to 28% (Peterson et al., 2026) and is underlain by sedimentary lithologic units primarily consisting of sand and clay (Szabo et al., 1988). Highly weathered, easily erodible soils have resulted in severe channel incision in the lower half of the watershed. This watershed is completely forested, with a historic forest structure of mixed oaks, hickory, and pine species (Griffith et al., 2001), but management for rotational silvicultural harvest has shifted the community towards uplands of predominantly pine species and riparian areas with mixed gum, oak, holly, sycamore, and ironwood species (Plont et al., 2026).

2.2 Hydrogeomorphic Features (HGFs)

To characterize river corridor structure within and across our watersheds, we delineated each watershed into distinct hydrogeomorphic features following Peterson et al. (2025). HGFs integrate topographic, geologic, and vegetative characteristics across compartments of the entire river corridor, rather than focusing only on the stream channel (Peterson et

https://doi.org/10.5194/egusphere-2026-4201
Preprint. Discussion started: 27 July 2026

al., 2025). First, we identified archetypical valley shapes within each of our study watersheds. Next, within these valley types, we defined watershed-specific HGFs based on field observations of structural characteristics of the river corridor that would potentially influence hydrologic connectivity and storage, such as stream incision, local slope, or soil texture. We outline the primary structural differences between these valley types and HGFs in Figure 2. Further, while these HGFs were assigned specifically to each watershed, they provide an opportunity to study hydrologic processes as a function of HGF regardless of which physiographic region a study is located within.

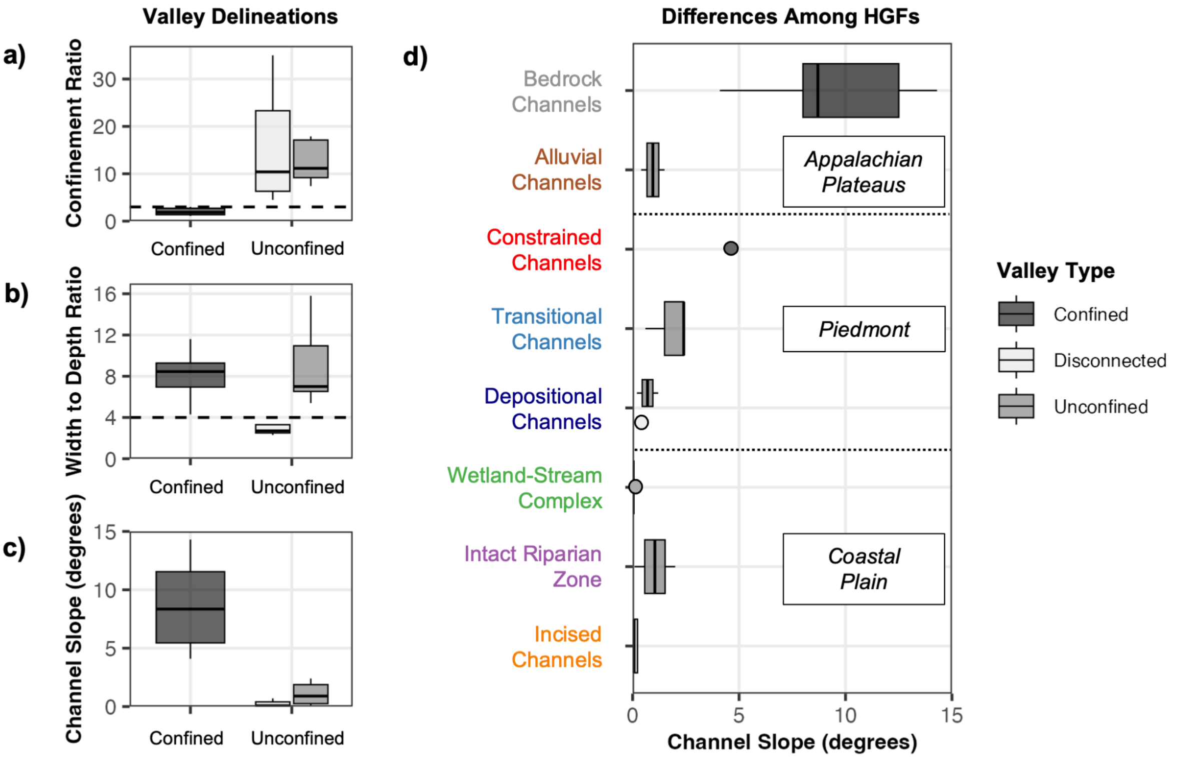

Figure 2: (a-b) The topographic valley-bottom metrics used to delineate valley types. (a) indicates the valley confinement ratio as the ratio between valley width and bankfull channel width. The threshold for confined valleys is marked by the dashed line. (b) indicates the channel width:depth, and the threshold for disconnected valleys is marked by the dashed line. (c-d) Channel slope as an example topographic metric to demonstrate differences between valley types (c) and HGFs (d). HGFs are grouped by watershed (dotted lines) and colored according to overarching valley type (see legend). HGFs with only one observation are indicated by points rather than boxes.

We defined three overarching valley types across our three watersheds based on valley and channel cross-sections extracted from digital elevation models (DEMs). First, valleys were split into either confined or unconfined based on the ratio of the valley width and bankfull channel width (*sensu* Montgomery & Buffington, 1998; Fryirs & Brierley, 2018). Here, we used a threshold of a confinement ratio ≤ 3, which is equivalent to the channel comprising 1/3 or less of the entire valley, regardless of overall channel or valley size (Fig. 2a). Further, within unconfined valleys, we identified disconnected valleys as those with severe incision that would reduce channel access to riparian zones and floodplains (*sensu* Peterson et al., 2025;

https://doi.org/10.5194/egusphere-2026-4201
Preprint. Discussion started: 27 July 2026

Rosgen, 1994). Here, we used a threshold of width:depth ≤ 4, which is equivalent to all channels less than 2 m wide containing at least 0.5 m of incision (Fig. 2b). It is important to note that while these three valley types are treated as distinct in this study, all disconnected valleys are otherwise unconfined; confined valleys cannot be disconnected in our categorization. These valley types also span our three research watersheds, and subsequent HGFs are defined within the context of their valley type. For example, the majority (n = 5) of monitoring locations in the Appalachian Plateaus watershed were confined valley types, and the majority (n = 4) of monitoring locations in the Coastal Plain were disconnected valley types. The Piedmont watershed was the only watershed with all three valley types present.

In the Appalachian Plateaus, we identified two distinct HGFs: (i) bedrock channels, and (ii) alluvial channels (Fig. 1c). Bedrock channels were all located in confined valley types, predominantly in the high elevation upper portions of the steam network (Fig. 1c), and comprised nearly 75% of the total network length. These HGFs were defined by exposed bedrock streambeds, little substrate accumulation, steep hillslopes, and thin, stony riparian soils that were predominantly organic horizons. This HGF also contained the majority of cave-springs and spring discharges in the watershed. Taken together, we expected that this HGF would have a low storage capacity with moderate connectivity (Table A1). Conversely, alluvial channels were dominant in the lower portions of the network closer to the watershed outlet (Fig. 1c), located in unconfined valley types, and made up over 25% of the total network length. These HGFs were defined as lower-gradient channels with finer substrates and sediment accumulation as well as well-developed, deep riparian soils. As a result, we predicted this HGF to have moderate storage capacity and low connectivity (Table A1).

In the Piedmont, we delineated the network into three HGFs: (i) constrained channels, (ii) transitional channels, and (iii) depositional channels (Fig. 1d). Constrained channels were defined as portions of the network located in confined valley types, with steep slopes and little soil accumulation. These HGFs made up 34% of the total network length, and we predicted they would represent regions of low storage and moderate connectivity (Table A1). Transitional channels were located in unconfined valleys, often in the middle reaches of the network (Fig. 1d), and were defined by increased riparian zone development with coarse stream sediment and soil textures. These HGFs comprised 36% of the total network length, and we predicted they would have moderate storage and low connectivity (Table A1). Finally, depositional channels were located in the lower portions of the network closest to the watershed outlet (Fig. 1d), and made up 30% of the total network length. While all three of the depositional channels HGFs were located in generally unconfined valleys, the most downstream site was classified as a disconnected valley type due to channel incision. Depositional channels HGFs were defined as wide, densely-vegetated riparian zones with low stream gradients and meandering channels. As such, we expected the depositional channels to have high storage and low connectivity (Table A1).

In the Coastal Plain, we delineated the network into three HGFs: (i) wetland-stream complexes, (ii) intact riparian zones, and (iii) incised channels (Fig. 1e). These HGFs were the same as documented in Peterson et al. (2025), where the HGF framework was developed in the same physiographic province. Wetland-stream complexes were located in unconfined valleys and defined as low-gradient reaches with riparian wetlands located adjacent to the channel. These HGFs comprised only 13% of the total network length, and we predicted them to have high storage and high connectivity (Table A1). Intact riparian zones

https://doi.org/10.5194/egusphere-2026-4201
Preprint. Discussion started: 27 July 2026

were also located in unconfined valley types and were defined as channels with distinct banks and evidence of over-bank flows into the riparian zone, making up 33% of the total network length. Both wetland-stream complexes and intact riparian zones were primarily concentrated in the upper reaches of the network (Fig. 1e). We expected the intact riparian zones to have moderate storage and high connectivity (Table A1). Finally, incised channels were located in disconnected valley types, predominantly in the lower half of the network (Fig. 1e), and were defined as deeply entrenched channels (i.e., > 0.5 m of incision; up to 2 m) that had lost access to the riparian zone. These HGFs comprised 54% of the total network length, and we predicted that they would have low storage and high connectivity (Table A1).

2.3 Hydrologic Monitoring Instrumentation

We instrumented each watershed with a network of surface and groundwater monitoring sensors to quantify hydrologic connectivity across space and time. Each watershed consisted of 20 water presence/absence sensors to quantify network length (hereafter, L; see Peterson et al., 2026 for more information), and seven long-term monitoring locations (hereafter, LTMs) distributed throughout the network to measure in-stream water level at the channel thalweg. Additionally, at three LTMs in each watershed, we installed groundwater monitoring wells perpendicular to the stream in the adjacent riparian zone to quantify groundwater table dynamics. All sensors collected data across the approximately two-year study period and logged at concurrent 15-minute intervals starting in Aug. 2022 through the spring of 2024, and then logged at concurrent hourly intervals from the spring of 2024 through Sep. 2024.

LTMs were distributed throughout each network to capture a gradient of drainage area accumulation, as well as to target the confluences of two major tributaries in each watershed (for more information on these locations, see Plont et al., 2026). All wells were instrumented with unvented Onset HOBO U20L pressure transducers (Onset Corporation, Massachusetts, USA). Groundwater monitoring wells were hand-augered during the dry season to depths of refusal, and installed such that the well was screened from the bottom to within 10 cm of the ground surface. Approximately every four months, we downloaded and relaunched all sensors and collected manual water level measurements. Further, in the winter of 2024, every location was manually surveyed using a laser level to measure both relative distances and depths of all wells, as well as absolute elevation of the transect.

We converted pressure transducer data to water elevation (m.a.s.l.) following Peterson et al. (2025). In short, we converted gage pressure to relative water level using the specific weight of water and corrected for local barometric pressure, which we collected concurrently using an additional, above-ground HOBO U20 pressure transducer near each watershed outlet. We then used the surveyed elevation data to convert water level to water elevation such that we could compare absolute elevation across both surface and groundwater wells in the same transects. These water elevation data were used for both water table slope and hysteresis calculations as well as recession analyses. Additionally, at each watershed outlet, we built a stage-discharge rating curve using manual measurements of discharge (Q) to estimate continuous discharge at 15-minute intervals for the duration of the study (for more information, see Plont et al., 2026).

https://doi.org/10.5194/egusphere-2026-4201
Preprint. Discussion started: 27 July 2026

2.4 Analyses

To compare storage and connectivity dynamics across physiographic regions, we calculated proxies specific to each of our scales of interest. At the watershed scale, we operationalized storage as streamflow recession slope (hereafter, b_Q) and connectivity as the relationship between discharge and network length. At the HGF scale, we operationalized storage as water level recession slope (hereafter, b_{WL}) and connectivity as groundwater-surface water interactions between the stream channel and riparian zone.

We quantified recession behavior by calculating the slope of event-scale water level and discharge recession following Jachens et al. (2020) and Vogel & Kroll (1992) as a proxy for storage in each watershed,. In short, we delineated all storm events for the two water-year study period based on Q at the outlet and extracted all water level and Q values during these events at an hourly resolution. We excluded any events that had multiple peaks from this analysis due to the complexity of calculating recession for these events, resulting in a final recession dataset of n = 39 events for the Piedmont watershed, n = 46 for the Appalachian Plateaus watershed, and n = 47 events for the Coastal Plain watershed. We then filtered our hourly data to only include periods where the derivative of water level (or Q) was decreasing (i.e., true recession; Tashie et al., 2020). We then plotted log-transformed water level (or Q) against its negative derivative (-dWL/dt or -dQ/dt), and extracted the slope (b) of the linear regression of the resulting point cloud as a measure of recession nonlinearity. While many lumped event-scale recession analyses utilize daily water level or Q data (e.g., Tashie et al., 2020; Dralle et al., 2017), in our small watersheds, recession events were often less than one day, so we utilized hourly data to provide a more robust analysis of our systems.

Using these recession slope values, we were then able to classify recession behaviors. Based on previous studies of Q recession across watersheds globally, $b_Q \geq 1$ generally indicates a more nonlinear recession, where streamflow initially recedes quickly following an event and then rapidly slows down (Harman et al., 2009, Tashie et al., 2020). Therefore, higher recession slopes suggest storage releases from more transient zones that can be depleted quickly. Recession slopes $b_Q < 1$ generally indicate more linear recession, where streamflow recedes more slowly and the rate of recession does not change. As such, lower recession slopes suggest releases from more stable storage zones. These thresholds were used to interpret the recession behaviors across events in our three research watersheds.

We then compared network extent dynamics across watersheds by calculating the slope of the relationship between L and outlet Q (β; Godsey & Kirchner, 2014) as a proxy for watershed-scale longitudinal connectivity. Details of this analysis in these three watersheds can be found in Peterson et al. (2026). Briefly, we identified representative reach lengths corresponding to each water presence/absence sensor, and calculated instantaneous network length L as the sum of all reaches with sensors recording wet conditions. Here, we area-normalized both Q and L observations by dividing by watershed area to provide more comparable values across the three watersheds of different sizes and network structures. We extracted the network expansion exponent, β, as the slope of the power-law relationship between L and Q, where β closer to 0 represent stable networks that are not sensitive to changes in Q, and β closer to 1 represent dynamic networks where L responds to changes in Q. It is worth noting that β derived from our sensor-derived L measurements should be interpreted as minimum

https://doi.org/10.5194/egusphere-2026-4201
Preprint. Discussion started: 27 July 2026

estimates of network elasticity, as sensors can only detect water presence within the instrumented network extent and may not capture expansion into ephemeral headwater reaches during high-flow events.

We characterized stream channel hydrologic state (i.e., lateral gain or loss) by calculating water table slope between the in-stream and riparian monitoring wells following Peterson et al. (2025) as a proxy for stream-riparian connectivity. We used water elevation data to calculate the vertical difference in the potentiometric surface between the surface water and groundwater well (m), and then divided this difference by the linear surface distance between the wells (m) to calculate water table slope. This slope was then interpreted as stream channel hydrologic state, where positive values suggest a hydraulic gradient moving towards the stream and indicate gain from the riparian zone, and negative values suggest a gradient away from the stream and indicate loss to the riparian zone. We aggregated these data to daily, monthly, and annual timescales to evaluate how dynamic gain/loss conditions varied across both time and space.

We quantified the magnitude and direction of connectivity between stream channels and riparian zones by calculating hysteresis index (hereafter, HI) at the event-scale between stream and riparian monitoring wells following Cain et al. (2025) and Zuecco et al. (2016). Using the complete dataset of events delineated for study period (n = 62, 63, and 77 for the Piedmont, Appalachian Plateaus, and Coastal Plain watersheds respectively), we extracted paired surface water and groundwater elevation data for individual events and normalized them to the range of values observed in each well for each event. We then split data into rising limb and falling limb series based on the stream channel relative elevation and calculated the definite integral of both limbs. We then subtracted the falling limb integral from the rising limb to calculate an absolute HI and hysteresis pattern, where HI $>$ 0 indicates clockwise hysteresis (faster groundwater response) and HI $<$ 0 indicates counterclockwise hysteresis (faster surface water response). HI $\approx$ 0 indicates either complex or no hysteresis; these patterns were identified by the ratio of counterclockwise and clockwise loops. Further, we calculated the absolute value of HI (hereafter, HI magnitude) as a measure of stream-riparian connectivity regardless of direction. It is worth noting that while HI is a measure of the relative timing of event responses (i.e., near-zero corresponds to more similar timing) and can be influenced by the storage state of the watershed, we interpret this relative timing as indicative of relative stream-riparian connectivity rather than actual fluxes. We expect that more similar responses in groundwater and surface water pools (i.e., low HI) suggest greater connectivity, as event signals propagate quickly through both pools.

To compare storage and connectivity metrics, we classified HGFs into high or low storage and connectivity using water level recession slopes and HI magnitudes. We defined the thresholds for high and low storage/connectivity based on potential ranges of values. For example, while there is no documented threshold between linearity and nonlinearity for recession slope (given that b is not conserved between Q and WL recession; Jachens et al., 2020), we defined a threshold of 2 based both on the range our individual event recessions and comparisons between Q and WL recession at the watershed outlets. As such, we defined water level recession slopes (b_{WL}) < 2 as indicative of higher relative storage, and b_{WL} > 2 as indicative of lower, more transient relative storage. Similarly, we set the threshold for HI magnitude as 0.5, given that HI ranges between 0 and 1 based on the area under the curve as well as our observations. Here, we defined HI magnitude < 0.5 as more similar

https://doi.org/10.5194/egusphere-2026-4201
Preprint. Discussion started: 27 July 2026

event responses and therefore greater stream-riparian connectivity, and HI magnitudes > 0.5 as more dissimilar event responses and therefore lower stream-riparian connectivity.

3 Results

3.1 Watershed storage and stream-riparian connectivity at the watershed outlet varied across landscapes

Using streamflow recession slope (b_Q) as a proxy for watershed storage, we observed key differences across our three study watersheds. Our highest-relief watershed, the Appalachian Plateaus, had the highest observed recession slope (b_Q = 1.28) of all three watersheds. Conversely, the Piedmont and Coastal Plain watersheds had very similar recession slopes (b_Q = 0.74 and 0.76, respectively; Fig. 3a). Therefore, the Appalachian Plateaus watershed exhibited more transient, less stable storage as evidenced by its relatively high recession slope. In contrast, b_Q > 1 indicated that the Piedmont and Coastal Plain watersheds had a more linear recession behavior, suggesting higher storage in more stable storage zones.

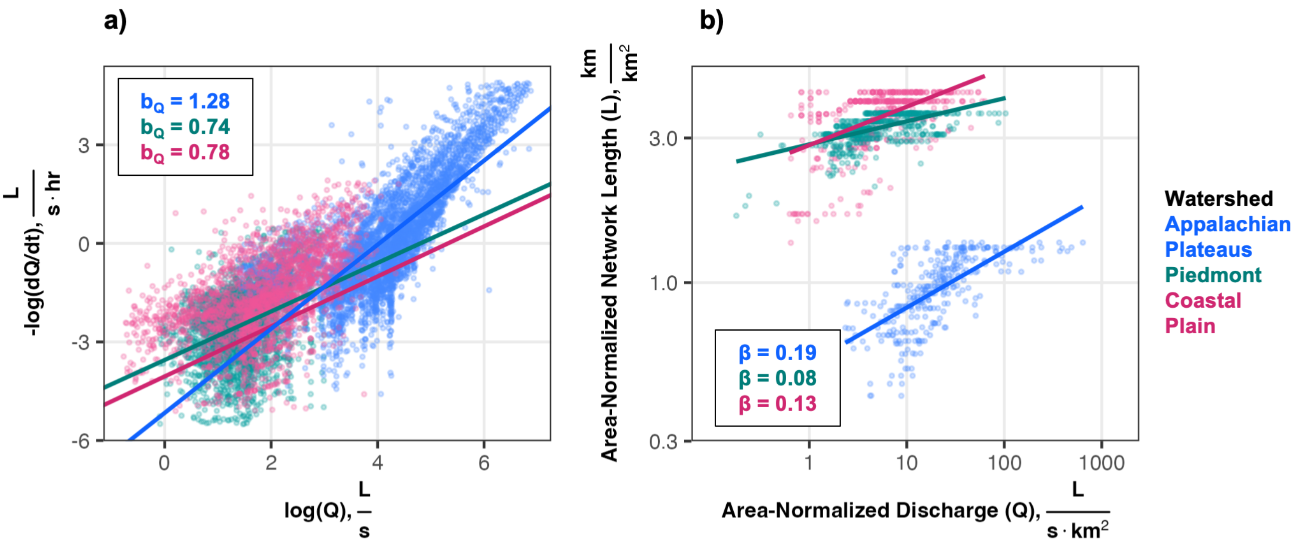

Figure 3: Storage and connectivity relationships at the watershed-scale for our three research watersheds. (a) recession analysis using Q at the outlet of each watershed, where each point is a 15-minute interval observation of log(Q) and -log(dQ/dt) during a storm event. Lumped recession slopes (b_Q) are included at the top left of the plot and are indicated by solid regression lines. (b) the relationship between watershed area-normalized outlet Q and watershed area-normalized network length (L). The slope of the log-log relationship between Q and L (β) are included in the bottom left of the plot, and are indicated by solid regression lines.

Stream network connectivity results indicate subtle differences in the magnitude of network expansion and contraction between watersheds. Using watershed-normalized Q-L relationships and the expansion exponent β, we found that the Appalachian Plateaus watershed was the most dynamic of the three (i.e., the largest β; Fig. 3a), and the Piedmont watershed was the most stable (smallest β; Fig. 3a). In the Appalachian Plateaus, area-normalized network length ranged from 0.08 to 1.36 km·km^{-2} across events, and the watershed had a β of 0.19 (Fig. 3b). Meanwhile, the Coastal Plain watershed normalized

https://doi.org/10.5194/egusphere-2026-4201
Preprint. Discussion started: 27 July 2026

network length ranged from 0.4 to 4.25 km·km^{-2} and had an expansion exponent of 0.13 (Fig. 3b). The Piedmont watershed had an expansion of exponent of 0.07, yet the normalized network length was generally comparable to the Coastal Plain, ranging from 2.33 to 3.62 km·km^{-2} (Fig. 3b).

3.2 Storage is related to river corridor structure

Storage, as assessed as water level recession slope (b_{WL}), was variable across HGFs. Across our eight HGFs, we found that the wetland stream complex and intact riparian zone HGFs, both of which were located in the Coastal Plain watershed in unconfined valley types, exhibited the most nonlinear recession (b_{WL} = 3.22 and 3.10 respectively; Fig. 4f-g) and are more likely to be driven by transient storage releases. Conversely, we observed the lowest water level recession slopes in the depositional channels in the Piedmont (b_{WL} = 0.17; Fig. 4e) and incised channels in the Coastal Plain (b_{WL} = 0.22; Fig. 4h), making these HGFs most likely driven by stable storage releases. For our other four HGFs, we had a distribution of moderate recession slopes; the constrained channels and transitional channels in the Piedmont had very similar b_{WL} values (b_{WL} = 1.28 and 1.26 respectively; Fig. 4c-d) that suggest more transient storage releases, and the alluvial channels and bedrock channels in the Appalachian Plateaus suggest more stable storage releases (b_{WL} = 0.51 and 0.36 respectively; Fig 4a-b). These moderate recession slopes spanned valley types, with similar b_{WL} values in both the unconfined and confined valleys of both watersheds. It is worth noting that while the threshold in b for linear to nonlinear is not fully consistent between streamflow recession and water level recession (Jachens et al., 2020), the magnitude of the threshold should be comparable. Further, we observed that there were event-scale heterogeneities in recession slopes across all HGFs, and while the lumped patterns were all observed to be positive, there were many sites with individual events that had significantly different slopes – even some negative slopes.

https://doi.org/10.5194/egusphere-2026-4201
Preprint. Discussion started: 27 July 2026

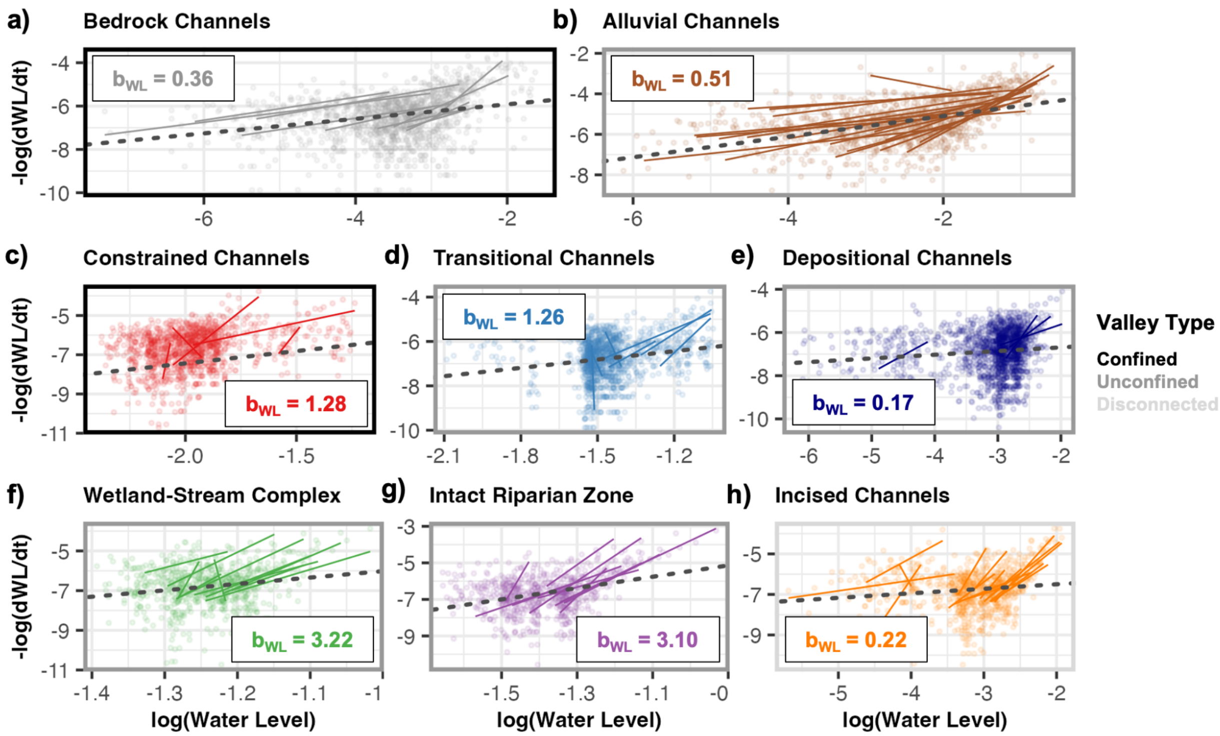

Figure 4: Water level recession slopes as a proxy for storage across our three valley types and eight HGFs. Each point represents a 15-minute interval measure of log(water level) and -log(dWL/dt) during an event. Events with significant linear relationships across the entire event are marked with colored lines, and significant overall lumped recession linear regressions are marked with grey dashed lines. The slope of the lumped regression (b_{WL}) is indicated in the corner of each plot. Panels (a-b) are in the Appalachian Plateaus watershed, (c-e) are in the Piedmont watershed, and (f-h) are in the Coastal Plain watershed. Panel borders indicate valley types (see legend for key).

At the individual site scale, we found that spatial variability in water level recession and subsequent storage differed among HGFs. The Appalachian Plateaus watershed was the most spatially consistent, with all individual LTMs displaying moderately linear recession slopes ranging from $b_{WL} = 0.25$ to 0.52 regardless of HGF or valley type (Table 1). The only outlier in this watershed was at the watershed outlet, where water level recession was highly nonlinear ($b_{WL} = 5.51$). Conversely, the Piedmont watershed was heterogeneous both across the watershed and within HGFs. Specifically in the transitional channels HGF, recession slopes in the mainstem ranged from $b_{WL} = 0.14$ to 1.26, whereas the recession slopes were highly consistent in the depositional channels HGF (b_{WL} ranged from 0.06 to 0.17; Table 1). Notably, both tributary LTMs in the Piedmont watershed had very similar negative recession slopes, contrasting with the entirely positive slopes observed in the mainstem. Finally, the Coastal Plain was the most spatially variable watershed, with many individual LTMs exhibiting greater differences in recession slope than the range of b_{WL} exhibited among HGFs. In the incised channels HGF specifically, recession slopes ranged from $b_{WL} = 0.22$ to 2.64 (Table 1). However, there was comparatively high variability in the degree of incision within

https://doi.org/10.5194/egusphere-2026-4201
Preprint. Discussion started: 27 July 2026

this HGF (Fig. A1), and we observed that lower recession slopes and therefore more stable storage releases were observed at LTMs with greater depths of incision.

Table 1: Summary of water level recession slopes within and across HGFs

Valley Type	HGF	LTM	WL Recession Slope (b)
Confined	Bedrock Channels	PRM11	0.52
		PRM15	0.32
		PRM19	**0.36**
		PRB01	0.25
		PRA01	0.37
	Constrained Channels	**TLM19**	**1.28**
Unconfined	Alluvial Channels	PRM01	5.51
		PRM06	**0.51**
	Depositional Channels	**TLM06**	**0.17**
		TLC01	-0.40
	Transitional Channels	TLM10	0.14
		TLM16	**1.26**
		TLA01	-0.41
	Intact Riparian Zone	WHA02	1.21
		WHM10	**3.10**
	Wetland-Stream Complex	**WHM12**	**3.22**
Disconnected	Depositional Channels	TLM01	0.06
	Incised Channels	WHM01	0.23
		WHM03	1.60
		WHM07	**0.22**
		WHB01	2.64

Note. LTMS in bold are the eight HGF locations used throughout the study. Water level recession slopes were significant for all LTMs ($p < 0.05$) except site TLM01 in the disconnected valley type depositional channels HGF.

3.3 Riparian connectivity was variable both across HGFs and seasons

Stream-riparian connectivity, as measured by the magnitude and direction of water table slope, fluctuated across watersheds and through time. In the Piedmont watershed, the stream channels in the constrained and transitional channels HGFs demonstrated primarily gaining conditions (i.e., positive water table slopes; Fig. 5a-b). In fact, the transitional channels HGF had some of the highest observed water table slopes (annual mean = 0.46; Table A2), indicating potential large groundwater discharges to the stream channel. However, some portion of this signal may be due to headcutting immediately

https://doi.org/10.5194/egusphere-2026-4201
Preprint. Discussion started: 27 July 2026

upstream of the sensor. Conversely, depositional channels in this watershed were predominantly losing throughout the study period (annual mean water table slope = -0.01; Table A2), though this was the only HGF in the Piedmont watershed to also indicate bidirectional flows (Fig. 5a). In the Coastal Plain, bidirectional flows were observed in all three HGFs, where all stream channels demonstrated gaining conditions and positive slopes in the wetter winter and spring seasons and negative slopes with losing conditions in the drier summer and fall seasons (Fig. 5c). However, the magnitude of these hydraulic gradients differed between HGFs, with the incised channels fluctuating from highly gaining (April mean water table slope = 0.05) to highly losing (October mean water table slope = -0.05) while the intact riparian zones and wetland-stream complex were predominantly losing with some event-based direction reversals (Table A2). Conversely, in the Appalachian Plateaus watershed, soil saturation was never documented in any of the riparian wells. This, paired with the shallow depths to bedrock across the watershed, suggests primarily losing conditions in the stream channel.

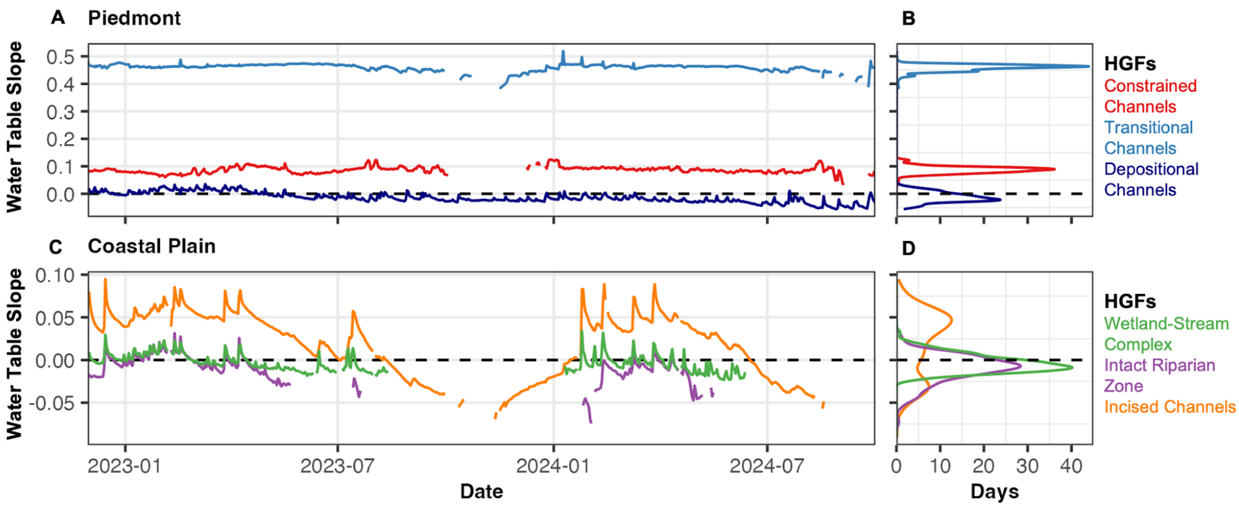

Figure 5: Hydraulic gradients for each HGF as average daily water table slope relative to the stream. Positive values indicate stream gain (i.e., gradient moving from riparian zone to stream channel), negative values indicate stream loss. Note that the Appalachian Plateaus watershed is not included in this analysis, as the riparian wells in this watershed did not have sufficient saturation to calculate water table slope.

Further, our stream-riparian hysteresis results further suggest that there are distinct patterns in the direction of hydrologic connectivity across HGFs. Following Cain et al. (2025), we interpret counterclockwise hysteresis as responses led by surface-water (i.e., surface water rises before groundwater) and clockwise hysteresis as responses led by groundwater (i.e., groundwater rises before surface water). In the Piedmont watershed, we observed an upstream-downstream gradient in hysteresis, where there was predominantly clockwise hysteresis in the constrained channels HGF, counterclockwise hysteresis in the depositional channels HGF, and a nearly even split between clockwise and counterclockwise in the transitional channels HGF (Fig. 6a). Conversely, all HGFs in the Coastal Plain watershed were dominated by counterclockwise hysteresis. While the incised channels HGF experienced a significant portion of clockwise hysteresis (33%; Fig. 6b), the majority of events in

https://doi.org/10.5194/egusphere-2026-4201
Preprint. Discussion started: 27 July 2026

all three HGFs exhibited surface water driven event responses. Again, there was no saturation in any riparian wells in the Appalachian Plateaus, so hysteresis could not be calculated.

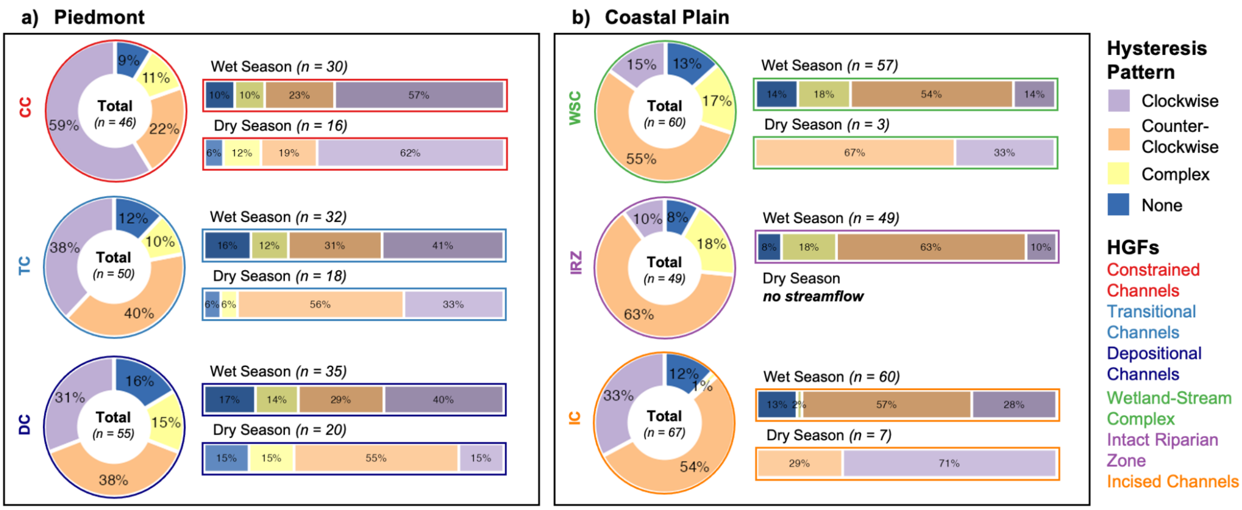

Figure 6: Hysteresis patterns across HGFs and seasons. Donut charts indicate the general hysteresis patterns (clockwise, counterclockwise, complex, or none) for all storms in each location to contextualize the general direction of hysteresis. Stacked bars indicate the splits of hysteresis directions between the wet (darker shades) and dry (lighter shades) seasons. See legend for more details. Note that the Appalachian Plateaus is excluded from this analysis, as the riparian wells in this watershed did not have sufficient saturation to measure hysteresis between the stream channel and the riparian zone.

Temporal patterns in hysteresis direction are also evident in our observations. In 3 of 5 HGFs, we observed a seasonal shift in the direction of hysteresis, though these patterns were not uniform. In the transitional channels and depositional channels in the Piedmont watershed, stream-riparian hysteresis was predominantly clockwise in the wet season (groundwater response) before shifting to counter-clockwise (surface water response) in the dry season (Fig. 6a). Conversely, the incised channels in the Coastal Plain were dominated by counter-clockwise hysteresis (surface water response) in the wet season, and shifted to clockwise (groundwater response) during the dry season (Fig. 6b). While we acknowledge that there are limitations to comparing hysteresis directions across uneven seasonal distributions of events, we expect that these patterns are representative of patterns and processes in each study system. Further, the limited number of dry season events for which hysteresis could be calculated also supports this seasonal shift; as events were delineated relative to outlet responses, hysteresis could not be calculated in the event of insufficient saturation in the riparian zone, suggesting that these dry-season events were often surface water driven.

3.4 Combining storage and connectivity metrics provides an opportunity to characterize interacting drivers of streamflow generation

To classify our HGFs based on hydrologic function, we compared water level recession slopes and HI magnitude to contextualize the interactions between storage and stream-riparian connectivity (Table 2). We found that half of the HGFs in

https://doi.org/10.5194/egusphere-2026-4201
Preprint. Discussion started: 27 July 2026

our study watersheds fell into the classification of high storage and high connectivity; the majority (n = 6) had high stream-riparian connectivity regardless of storage (Table 2). All three HGFs in the Piedmont watershed as well as the incised channels in the Coastal Plain fell into the high storage and high connectivity quadrant, while the intact riparian zones and wetland-stream complex HGFs in the Coastal Plain fell into the low storage and high connectivity quadrant (Table 2). Conversely, both HGFs in the Appalachian Plateaus watershed were located in the high storage and low connectivity quadrant, primarily as a function of the lack of observed stream-riparian connectivity in this watershed. Further, we did not observe any HGFs that exhibited low storage and low connectivity.

Table 2: HGF storage and stream-riparian connectivity proxies and classifications

Watershed	HGF	Recession Slope	Storage Classification	Mean HI Magnitude	Connectivity Classification
Appalachian Plateaus	Bedrock Channels	0.36	High	-	Low
	Alluvial Channels	0.51	High	-	Low
Piedmont	Constrained Channels	1.28	High	0.19 ± 0.14	High
	Transitional Channels	1.26	High	0.21 ± 0.15	High
	Depositional Channels	0.17	High	0.25 ± 0.27	High
Coastal Plain	Wetland-Stream Complex	3.22	Low	0.20 ± 0.14	High
	Intact Riparian Zone	3.10	Low	0.24 ± 0.15	High
	Incised Channels	0.22	High	0.24 ± 0.16	High

Note. Due to insufficient saturation in the riparian wells in the Appalachian Plateaus, HI magnitude could not be calculated, and stream-riparian connectivity is assumed low (given that streamflow persisted in the absence of riparian saturation).

4 Discussion

4.1 Outlet-scale patterns are a poor predictor of within-watershed dynamics of storage and connectivity

Watershed storage and stream-riparian connectivity dynamics highlight the inherent heterogeneity within three intensively-monitored watersheds. Patterns observed at watershed outlets reflect integration of patterns and processes that are observed at the smaller spatial scales nested within them. By classifying storage and connectivity dynamics exclusively based

https://doi.org/10.5194/egusphere-2026-4201
Preprint. Discussion started: 27 July 2026

on our outlet-scale results, these three watersheds are distinct from one another, and only align with some previous expectations of network dynamics. We observed the lowest storage observed in the watershed with the shallowest soils (Price, 2011), and the lowest longitudinal network connectivity in the watershed with the lowest relief (Jencso & McGlynn, 2011). In the Appalachian Plateaus, moderately high discharge recession slopes (b_Q = 1.28) suggest storage from more transient sources (Tashie et al., 2019). Further, this watershed's dynamic network (β = 0.19) paired with low normalized network lengths (Fig. 3) suggests moderately low network connectivity. Conversely, both the Piedmont and Coastal Plain's discharge recession slopes (b_Q = 0.74 and 0.76 respectively) indicate storage release from more stable sources (Vogel & Kroll, 1992; Tashie at al., 2019). These two high-storage watersheds, however, had divergent network connectivity dynamics; where a stable network (β = 0.08) paired with high normalized network lengths in the Piedmont suggests high connectivity, a moderately dynamic network (β = 0.13) with similarly high network lengths in the Coastal Plain indicated lower network connectivity (Fig. 3). Taken together, these outlet-scale results support our prediction that physical watershed template drives storage and connectivity dynamics.

However, our HGF-scale results indicate that storage and connectivity patterns at the watershed outlets were not reflective of patterns at the HGF scale. This difference was most pronounced in the Appalachian Plateaus watershed, as water level recession slopes throughout the watershed were highly consistent and suggested high storage with releases from stable sources (Table 1), while water level recession slope at the outlet suggested highly nonlinear recession from transient storage zones (b_{WL} = 5.51). We attribute this discrepancy as the influence of karst topography within this watershed. While there are confined valleys with little soil storage and steep slopes throughout, the abundance of cave-springs and large volumes of stable storage in highly conductive bedrock contributes to more linear water level recession moving upstream, similar to the findings in Sayama et al. (2011). Results from the Coastal Plain watershed also suggest variability in storage and connectivity dynamics that do not align with patterns at the outlet. All three HGFs in the Coastal Plain had consistently low HI magnitudes (< 0.24; Fig. A3) that suggest high stream-riparian connectivity throughout, regardless of HGF and valley type. Watershed storage was more complex, with water level recession slopes in the incised channels near the outlet suggesting high storage with releases from stable sources, while recession slopes further from the outlet suggest low re storage with releases from transient source areas. These findings contrast with observations at the outlet, where the Coastal Plain showed high storage and low network connectivity. Taken together, these results challenge conceptualizations of low-relief systems, where stream-riparian connectivity was universally high despite low gradients (Jencso & McGlynn, 2011) and storage was highest in incised channels (contrary to the findings in Kirker et al., 2025; Peterson et al., 2025).

Watersheds are recognized as integrating heterogeneity at intermediate scales to generate emergent patterns in hydrologic responses at watershed outlets (e.g., Harman et al., 2009; Jencso et al., 2009; McDonnell et al., 2007). Therefore, it is unsurprising that patterns in storage and connectivity at the watershed outlets do not map directly onto within-watershed patterns observed across HGFs. Instead, observations at individual HGFs represent smaller-scale contributions to conditions at the watershed outlet, but are also inherently integrated with dynamics of other HGFs as the stream network aggregates, transforms, and transports inputs. However, the patterns we observed do not match conceptualizations of scaling storage and

https://doi.org/10.5194/egusphere-2026-4201
Preprint. Discussion started: 27 July 2026

watershed heterogeneity. Several studies have documented that larger watersheds that integrate heterogeneity trend toward larger, more non-linear recession slopes as flowpaths and storage zones become more complex and distributed (e.g., Tashie et al., 2019, Harman et al., 2009, Clark et al., 2009). However, we observed the opposite pattern in two of our three watersheds. We found the watershed outlet recession slopes in the Coastal Plain and Piedmont were more linear than upstream locations in the same network. We interpret this pattern not as a contradiction to prior studies, but as further emphasis on the role of heterogeneity within watersheds. We expect that high storage and high connectivity river corridor structures near the watershed outlet bias these signals, given the additional heterogeneity in recession slopes observed within individual HGFs in both watersheds (Table 1). Our results further emphasize the importance of studying intermediate scales and "key compartments" (*sensu* Spence, 2010) of the river corridor to explain patterns at watershed outlets. HGFs provide the opportunity to investigate sites with similar physical characteristics to study interacting controls of storage and connectivity (*sensu* Peterson et al., 2025).

4.2 Storage and connectivity relationships did not align with existing expectations of geomorphic features, highlighting interactions between local and upstream controls

Storage and stream-riparian connectivity provide important context to interpret within-watershed hydrologic patterns, yet these two methods inherently integrate across different spatial scales. As streamflow and water level recession is measured in the stream channel, observed recession slopes reflect the active storage of all upstream storage zones. Even using our nested design, HGF-scale recession results are most directly measuring releases from all storage zones in their respective subwatersheds (*sensu* Clark et al., 2009) rather than isolating signals unique to an individual HGF. Conversely, our stream-riparian hysteresis and hydraulic gradient results characterize responses and patterns in both the stream channel and the adjacent riparian zones, reflecting both local and upstream controls on connectivity within the river corridor. Taken together, these techniques provide a complementary framework to characterizing hydrologic processes within and across watersheds.

In the Coastal Plain watershed, we had initially predicted that the presence of riparian wetlands and highly connected riparian zones would yield greater storage in the wetland-stream complex and intact riparian zone HGFs than the incised channels HGF (Table A1, Table 3). Many studies have highlighted the role that riparian wetlands play in providing surface and subsurface storage, and high storage capacity in these wetlands can modulate both high and low flows (e.g., McLaughlin et al., 2014; Kirker et al., 2025) and contribute stable, often bidirectional flows to downstream channels and nearby riparian zones (e.g., Peterson et al., 2025; Wegener et al., 2017). Similarly, previous studies have documented that highly connected riparian zones are also important storage zones, as these locations are often regions of groundwater recharge and bidirectional flows during storm events (e.g., Godsey & Kirchner, 2014; Larned et al., 2011; Ploum et al., 2021). However, both the wetland-stream complex and intact riparian zone HGFs water level recession slopes suggested relatively low storage from primarily transient storage zones (*sensu* Harman et al., 2009; Fig. 4). Further, both HGFs demonstrated predominantly losing channels (Fig. 5c) and surface water driven responses (Fig. 6b). Here, we expect that this low storage from transient zones paired with high stream-riparian connectivity is primarily the result of densely vegetated riparian zones with high evapotranspiration year-round that lower local water tables. Despite unconfined valleys yielding high storage potential (i.e., deep, coarsely grained and

https://doi.org/10.5194/egusphere-2026-4201
Preprint. Discussion started: 27 July 2026

organic soils, low relief; Zecharias & Brutsaert, 1988), evapotranspiration in riparian zones can reduce available storage and shift recession slopes to higher, more nonlinear values (e.g., Shaw & Rija, 2012; Tashie et al., 2019). Consequently, we expect that the dense coniferous vegetation in the riparian zone drive high evapotranspiration year-round in these two HGFs (Peterson et al., 2026), resulting in lowered riparian storage accessible to the stream, and yielding overall losing conditions. While these empirical results contradict the recession slopes in a hydrologic modelling study in this same research watershed (Kirker et al., 2025), these discrepancies likely arise from the same process at different scales; here, localized water table lowering reduces riparian storage, but at the larger scales modelled by Kirker et al. (2026), higher water tables contributed to increased resilience to drying likely due to higher storage.

In the Piedmont, we observed moderate storage and high stream-riparian connectivity in both the constrained and transitional channels HGF. Given the confined valley type and steeper slopes of the constrained channels compared to the increased riparian zone development and deeper soils in the transitional channels, we expected higher recession slopes and primarily surface water responses in the constrained channels, and lower recession slopes with groundwater responses in the transitional channels (Voegel & Kroll, 1992). Instead, we found that both the constrained and transitional channel HGFs were generally gaining and had similar, moderate water level recession slopes (b_{WL} = 1.28 and 1.26; Fig. 4). Further, the constrained channels were predominantly gaining channels with clockwise hysteresis responses, suggesting high stream-riparian connectivity with rapidly responding groundwater sources (Cain et al., 2025). The transitional channels demonstrated clockwise (rapid groundwater source) and counterclockwise (rapid surface water source) hysteresis in approximately equal frequency. We anticipate that the unexpectedly similar storage and connectivity dynamics in these two HGFs is not a function of valley type, riparian area, and potential storage. Rather, we posit the observed storage and connectivity dynamics reflect contributions from deeper groundwater sources that sustain and stabilize streamflows. Previous studies have documented that storage in permeable bedrock can outweigh the role of basin slope in regulating storage and contribute to more stable, linear recession dynamics (e.g., Sayama et al., 2011; Table 3). While the dominant lithologic units in the Piedmont watershed are not necessarily permeable, they are highly fractured due to their proximity to the Talladega fault (Cook, 1982; Kopaska-Merkel et al., 2000) and likely contribute preferential groundwater flow to the river corridor. As a result, we expect that these deeper groundwater flows contribute to the stream channel and provide storage in the constrained channels despite the apparent confined valley.

https://doi.org/10.5194/egusphere-2026-4201
Preprint. Discussion started: 27 July 2026

Table 3: Summary of potential controls, related proxies, and expected patterns for storage and connectivity at both the watershed and HGF scales

Scale	Potential Control	Proxy	Expectation for Storage		Expectation for Connectivity	
Watershed	Potential soil storage	Average Soil Depth	Deeper soils and coarser soil textures yield higher storage	*McNamara et al., 2011; Price, 2011*	n/a	
	Topographic gradient	Watershed relief	Steeper watersheds with permeable bedrock yield higher storage ***OR*** Steeper watersheds yield lower storage	*Sayama et al., 2011* *McGuire et al., 2005*	Greater topographic gradients yield higher connectivity	*Jencso & McGlynn, 2011; Prancevic & Kirchner, 2019*
	Geologic permeability	Regional lithology	More permeable lithologies (fractured or soluble units) yield higher storage	*Price, 2011*	n/a	
HGF	Potential soil storage	Average depth to bedrock	Deeper soils yield higher storage	*McNamara et al., 2011, Price, 2011*	Subsurface topography regulates connectivity such that higher connectivity occurs in locations with shallower soils	*Tromp-van Meerveld & McDonnell, 2006b*
		Primary soil texture	Coarser soil textures yield higher storage	*McNamara et al., 2011*	Coarser, more homogenous soil textures yield lower connectivity; heterogeneities like confining layers increase connectivity	*Zimmer & McGlynn, 2018; Ali et al., 2011*
	Riparian zone potential storage	Valley confinement ratio	Greater riparian zone potential storage (i.e., lower valley confinement ratios) yield increased storage	*Jencso et al,. 2010*	n/a	
		Riparian wetland storage	Presence of riparian wetlands and surface water pools yields increased storage	*Jones et al., 2018*	n/a	
	Preferential flowpath abundance	Karst topography	Increased preferential flowpath abundance yields higher storage	*Onda et al., 2001*	Increased preferential flowpath abundance yields higher connectivity	*Zimmer & McGlynn, 2018; Menichino & Hester, 2015*
	Topographic gradient	Channel slope	Steeper watersheds with permeable bedrock yield higher storage ***OR*** Steeper watersheds yield lower storage	*Sayama et al., 2011* *McGuire et al., 2005*	Greater topographic gradients yield higher connectivity	*Jencso & McGlynn, 2011*
	Channel incision	Width:Depth	Deeply incised channels yield decreased near-stream storage	*Peterson et al., 2025*	Deeply incised channels yield increased connectivity	*Peterson et al., 2025; Chen et al., 2020*

https://doi.org/10.5194/egusphere-2026-4201
Preprint. Discussion started: 27 July 2026

Altogether, our results highlight the linkages between storage and stream-riparian connectivity. Many studies have conceptualized storage and connectivity as hierarchical, where connectivity occurs as a function of available storage (e.g., Tetzlaff et al., 2014; Kirker et al., 2025). Further, many studies have only directly measured either storage or connectivity, rather than assessing both and their relationship (e.g., McNamara et al., 2011; Krakauer & Temimi, 2011; Tashie et al., 2019). Our results showcase why quantifying both storage and connectivity matters: storage- or connectivity-only lenses can mask upstream, smaller-scale controls on streamflow generation, such as evapotranspiration and deeper groundwater contributions. Further, our results emphasize the complex relationship between storage and connectivity; half of our HGFs demonstrated both high storage and high stream-riparian connectivity patterns, and an additional two exhibited high stream-riparian connectivity despite low storage. These results emphasize that storage and connectivity are distinct yet complementary, and must be considered in tandem to fully capture hydrologic patterns within and across watersheds.

4.3 HGF-scale results suggest that structural characteristics like incision interact to drive observable patterns

Specific river corridor structures (e.g., incision, riparian wetlands, soil confining layers; Table 3) disproportionately influence storage and connectivity dynamics in comparison to broader, watershed-scale controls. Here, one dominant control that emerged from our observations of HGF structures across watersheds was channel incision. We observed that disconnected valley types and HGFs defined by incised channels demonstrated both high storage (Fig. 4) and moderately high stream-riparian connectivity (Fig. 5, Table 2), which did not align with our expectations (Table A1). Previous studies using different methodologies had identified incised channels as zones of decreased storage but with high stream-riparian connectivity and predominantly gaining channels (e.g., Peterson et al., 2025; Kirker et al., 2025). In this study, we observed that these incised channels HGFs had very low water level recession slopes ($b_{WL} = 0.22$), suggesting high storage in more stable storage zones (Vogel & Kroll, 1992; Harman et al., 2009). Further, our results suggest that incised channels have moderately high connectivity. These HGFs shifted between gaining and losing throughout the year (Fig. 5), with streamflow coming from both upstream surface water and local groundwater sources (Fig. 6). Additionally, we found that this high-storage, moderately high-connectivity signal was mirrored in the disconnected valley type of the Piedmont watershed, where channel incision was also > 0.5 m and observed recession slopes and HI magnitudes were nearly identical to those in the incised channels (Table 2). We expected the physiographic differences between the Piedmont and Coastal Plain watersheds to drive differences in storage and stream-riparian connectivity (Table 3). Therefore, this high similarity between HGFs in two distinct watersheds demonstrates the disproportionate role of incision on storage and connectivity dynamics. Incision has been documented to homogenize urban landscapes (Van Meter et al., 2016; Vietz et al., 2016) and change the storage dynamics of riparian zones (e.g., Loheide & Booth, 2011; Turner at al., 2015). Therefore, we interpret these highly similar storage and connectivity dynamics in the incised channels and depositional channels as a function of channel incision and disconnected valley types.

Further, our results highlight that channel incision is a continuous process that generates gradients and threshold responses in watershed storage. We had a large number of individual LTMs within the incised channels HGF (n = 4), which was primarily due to the dominance of channel incision within the Coastal Plain watershed. However, unlike other HGFs, the

https://doi.org/10.5194/egusphere-2026-4201
Preprint. Discussion started: 27 July 2026

incised channels HGF demonstrated a large range of water level recession slopes (Table 1), suggesting heterogeneity in storage zones within this HGF. We anticipate that this variability is primarily a function of the degree of incision; while incised channels were defined as width:depth ratios corresponding to depths of incision > 0.5 m (Peterson et al., 2025; Rosgen, 1994), there was a large range in incision depth across this watershed (Fig. A1). The locations of the watershed outlet LTM and our stream-riparian well transect were the most incised, with channels incised nearly 2 m below the streambanks. These two locations were also the two most consistent and lowest water level recession slopes ($b_{WL} < 0.23$; Table 1), suggesting high storage from stable storage zones. On the contrary, the other two locations were incised less than 1 m below the streambank and had water level recession slopes which suggest more transient storage zones (which aligns with findings in the same watershed from Kirker et al., 2025).

We expect that these divergent results indicate a threshold response in storage – regions of minor to moderate channel incision likely reduce storage by decreasing overbank flows and groundwater recharge (e.g., Squillace et al., 1996; Hester et al., 2020; Zimmer & McGlynn, 2018), resulting in more nonlinear recession from transient storage zones. However, once the channel has been incised severely, the channel intersects the permanent water table (e.g., Peterson et al., 2025) and has access to more stable, high storage zones which contributes to lower recession slopes, higher stream discharges (e.g., Chen et al., 2020), and more stable streamflows with reduced drydown events (e.g., Kirker et al., 2025; Peterson et al., 2026). Taken together, these results highlight the complex interactions of processes driving storage and connectivity, and suggest that there are thresholds in river corridor structure that generate distinct, homogenous hydrologic responses.

5 Conclusions

We used a dense network of surface water and groundwater monitoring sensors to measure watershed storage and riparian connectivity in three watersheds across a physiographic gradient in the southeastern US. Further, we identified key river corridor structural characteristics (here, hydrogeomorphic features, HGFs) to investigate river corridor-scale heterogeneity in storage and stream-riparian connectivity, as well as to characterize key features that would drive hydrologic patterns outside of larger watershed contexts. Our study found that storage and connectivity were distinct yet complimentary, and patterns in water level recession (as a proxy for storage) and proxies for connectivity at watershed outlets did not align with storage and connectivity patterns at subsequent HGF scales within watersheds. Further, we observed that patterns in storage – particularly in wetlands, riparian zones, and incised channels – did not always align with previous conceptualizations of geomorphic features, suggesting that interactions within the river corridor drive observable patterns in water level recession and storage. Additionally, our results suggest that channel incision homogenizes landscapes regardless of watershed context and displays threshold behaviors that shape storage and connectivity dynamics within watersheds. While this work was limited to three intensively monitored watersheds, we expect that our combination of storage and connectivity metrics as well as use of HGFs can be applied across watersheds regardless of landscape setting to identify key structural features that both generate watershed heterogeneity and hydrologic patterns.

https://doi.org/10.5194/egusphere-2026-4201
Preprint. Discussion started: 27 July 2026

Appendix A

Table A1: Summary of HGF delineation criteria, characteristics, and storage and connectivity predictions

Watershed	HGF	Valley Type	Delineation Criteria	HGF Characteristics	Storage Prediction	Connectivity Prediction
Appalachian Plateaus	Bedrock Channels	Confined	Bedrock streambeds with little to no sediment accumulation	Steep in-channel and local slopes, thin, mostly organic soils, high density of cave-springs	Little soil storage yielding **low storage capacity**	High preferential flow abundance and steep slopes yielding **moderate connectivity**
	Alluvial Channels	Unconfined	Lower-gradient channels with sediment accumulation	Fine substrate, well-developed, deep, and coarse-textured riparian soils, wider riparian areas	Increased soil storage yielding **moderate storage capacity**	Lower slopes and coarser soil textures yielding **low connectivity**
Piedmont	Constrained Channels	Confined	Steep slopes with shallow soils in V-shaped valleys	Steep in-channel and local slopes, limited riparian areas, thin fine-textured soils	Limited soil storage yielding **low storage capacity**	Steeper slopes and finer soil textures yielding **moderate connectivity**
	Transitional Channels	Unconfined	Coarse stream sediments and moderate riparian area widths	Coarser-textured and deeper soils, moderate slopes, located in middle of the network	Increased riparian area width yielding **moderate storage capacity**	Moderate slopes and coarser soil textures yielding **low connectivity**
	Depositional Channels	Unconfined/ Disconnected	Wide riparian areas and shallow slopes	Meandering channels, deep and finer-textured soils	Deep soils in wide riparian areas yielding **high storage capacity**	Shallow slopes yielding **low connectivity**
Coastal Plain	Wetland-Stream Complexes	Unconfined	Lower-gradient channels with adjacent riparian wetlands	Wide riparian areas, shallow slopes, deep and primarily organic soils	Deep soils and riparian wetlands yielding **high storage capacity**	Finer soil textures and low slopes yielding **high connectivity**
	Intact Riparian Zones	Unconfined	Wide riparian zones with evidence of over-bank flows	Deep, primarily organic soils, moderate-gradient channels with distinct banks	Deep soils and wide riparian areas yielding **moderate storage capacity**	Finer soil textures and low slopes yielding **high connectivity**
	Incised Channels	Disconnected	Deeply entrenched channels with limited access to riparian areas	High near-stream gradients, higher slopes, fine-textured soils	Lack of access to riparian area yielding **low storage capacity**	High near-stream gradients yielding **high connectivity**

https://doi.org/10.5194/egusphere-2026-4201
Preprint. Discussion started: 27 July 2026

Figure A1: Depths of channel incision across the four LTMs in the Coastal Plain incised channel HGF. Each profile is colored by LTM. Cross-section position of 0 indicates the channel thalweg.

Table A2: Monthly and annual average water table slope across HGFs

HGF	Jan	Feb	Mar	Apr	May	Jun	Jul	Aug	Sep	Oct	Nov	Dec	*Annual*
Depositional Channels	0.00	0.00	0.00	-0.01	-0.02	-0.02	-0.02	-0.02	-0.02	-0.02	-0.01	-0.01	*-0.01*
Transitional Channels	0.47	0.46	0.47	0.47	0.47	0.46	0.46	0.45	0.45	0.44	0.44	0.46	*0.46*
Constrained Channels	0.09	0.08	0.09	0.09	0.09	0.08	0.09	0.09	0.09	0.07	0.09	0.09	*0.09*
Incised Channels	0.03	0.05	0.05	0.05	0.03	0.01	-0.01	-0.02	-0.04	-0.05	-0.05	0.01	*0.02*
Intact Riparian Zone	0.00	-0.01	-0.01	-0.01	-0.03	–	-0.03	–	–	–	–	-0.01	*-0.01*
Wetland-Stream Complex	0.00	0.00	0.00	0.00	-0.01	-0.01	-0.01	-0.01	–	–	–	0.00	*0.00*

https://doi.org/10.5194/egusphere-2026-4201
Preprint. Discussion started: 27 July 2026

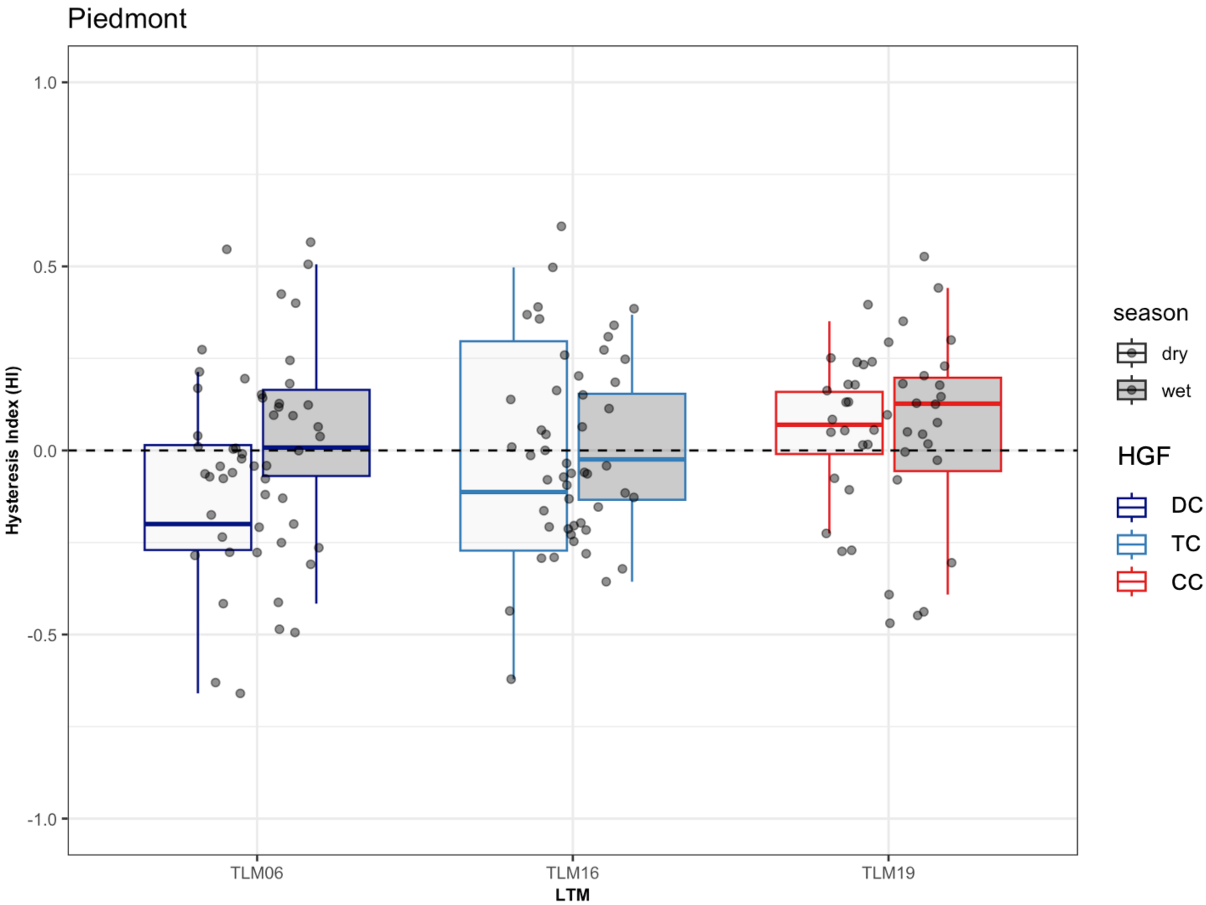

605 **Figure A2: Hysteresis Index (HI) for all storm events at each LTM in the Piedmont watershed, aggregated by wet and dry season. Individual events are indicated by jittered points. Positive values indicate clockwise hysteresis, and negative values indicate counterclockwise.**

https://doi.org/10.5194/egusphere-2026-4201
Preprint. Discussion started: 27 July 2026

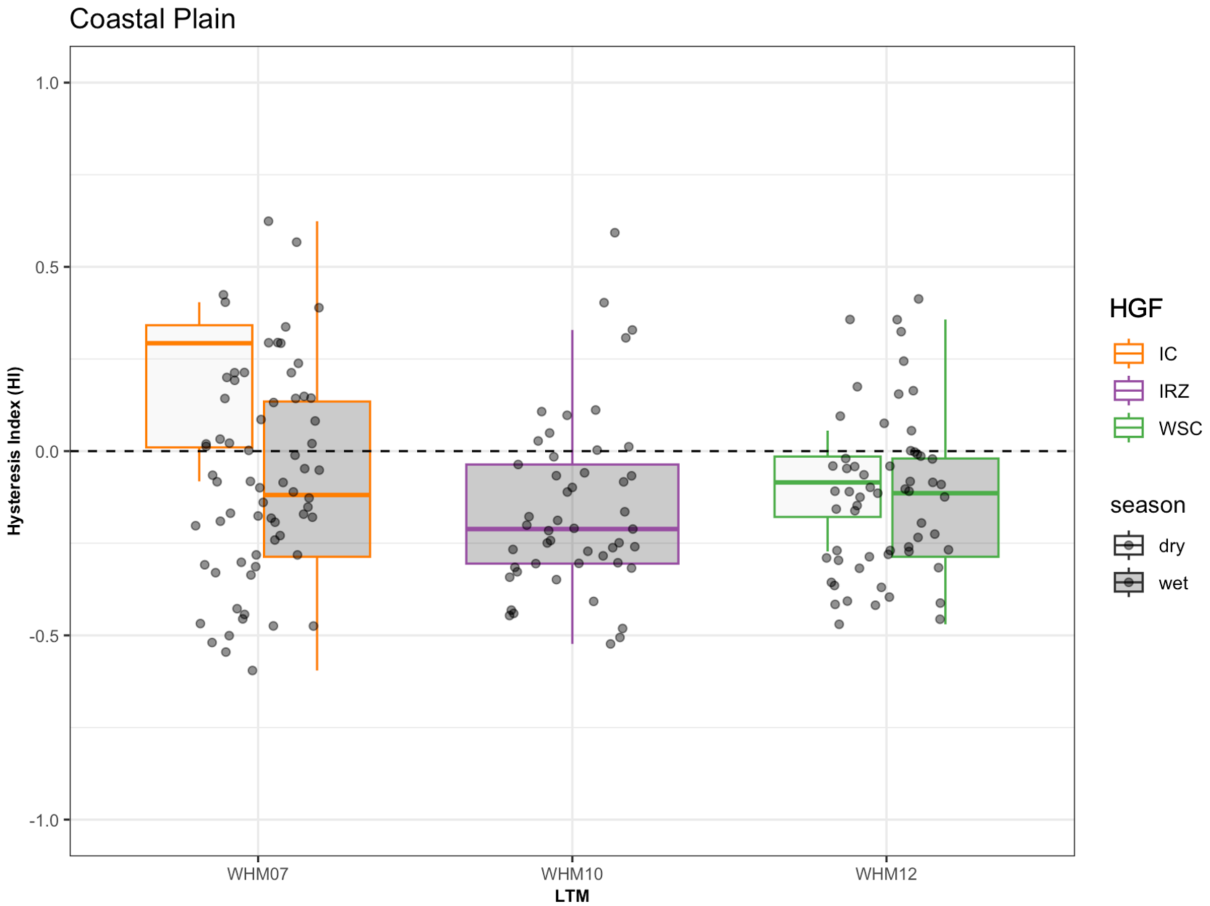

610 **Figure A3: Hysteresis Index (HI) for all storm events at each LTM in the Coastal Plain watershed, aggregated by wet and dry season. Individual events are indicated by jittered points. Positive values indicate clockwise hysteresis, and negative values indicate counterclockwise.**

615 **Code and data availability**

All data used in this study are available through CUAHSI HydroShare in the public AIMS Data group (https://www.hydroshare.org/group/247) and are linked in the references below. Additional information about these and co-collected data can be found in Plont et al. (2026). Code for respective analyses will be hosted on a public repository upon publication.

https://doi.org/10.5194/egusphere-2026-4201
Preprint. Discussion started: 27 July 2026

Author contributions

DMP and CNJ conceptualized this work with assistance from SJP, SEG, and CLA. CNJ, CLA were primarily responsible for funding acquisition, project administration, and supervision with assistance from DMP, SJP, SEG, and ASW. DMP was primarily responsible for fieldwork, data collection, and data curation with assistance from KRZ, SJP, CNJ, and CLA. DMP was primarily responsible for methodology, formal analysis, and visualization with assistance from CNJ, SJP, and SEG. DMP was primarily responsible for writing the initial and final draft of this manuscript, with all coauthors contributing to revising and editing manuscript drafts.

Competing interests

The authors declare there are no conflicts of interest or competing interests for this manuscript.

Acknowledgements

The authors would like to thank the US Forest Service, the Weyerhaeuser Company, and private landowner John Gully for their management, support, and access to the research watersheds. The authors would also like to thank Dr. Jami Nettles, Dr. Ashleigh Kirker, Chelsea Smith, Helen Czech, Patience Knight, Michelle Wolford, Justus King, Caroline Anscombe, Jacob Ackerman, Dr. Shannon Speir, Dr. Charlie Bond, Dr. Andrielle Larissa Kemajou Tchamba, Lidia Molina Serpas, Jasmine Morejon, and many other friends and colleagues for their help with instrument maintenance, site management, and fieldwork. The authors received support from the AIMS Project (Aquatic Intermittency effects on Microbiomes in Streams; funded by the National Science Foundation, Award Number 2019603), the University of Alabama Graduate School, and the Alabama Water Institute. Ward and Peterson were supported by the U.S. Department of Energy, Office of Science, Biological and Environmental Research, Environmental System Science Program through the Watershed Dynamics and Evolution (WaDE) Science Focus Area at Oak Ridge National Laboratory (ORNL); ORNL is managed by UT-Battelle LLC for the U.S. Department of Energy under contract DE-AC05-00OR22725.

References

Ali, G. A., L'Heureux, C., Roy, A. G., Turmel, M.-C., and Courchesne, F.: Linking spatial patterns of perched groundwater storage and stormflow generation processes in a headwater forested catchment, Hydrological Processes, 25, 3843–3857, https://doi.org/10.1002/hyp.8238, 2011.

Allen, G. H., Pavelsky, T. M., Barefoot, E. A., Lamb, M. P., Butman, D., Tashie, A., and Gleason, C. J.: Similarity of stream width distributions across headwater systems, Nat Commun, 9, 610, https://doi.org/10.1038/s41467-018-02991-w, 2018.

https://doi.org/10.5194/egusphere-2026-4201
Preprint. Discussion started: 27 July 2026

Barnard, H. R., Graham, C. B., Van Verseveld, W. J., Brooks, J. R., Bond, B. J., and McDonnell, J. J.: Mechanistic assessment of hillslope transpiration controls of diel subsurface flow: a steady-state irrigation approach, Ecohydrology, 3, 133–142, https://doi.org/10.1002/eco.114, 2010.

Bracken, L. J., Wainwright, J., Ali, G. A., Tetzlaff, D., Smith, M. W., Reaney, S. M., and Roy, A. G.: Concepts of hydrological connectivity: Research approaches, pathways and future agendas, Earth-Science Reviews, 119, 17–34, https://doi.org/10.1016/j.earscirev.2013.02.001, 2013.

Cain, M. R., Hixson, J. L., Jones, C. N., Rhoads, B. L., and Ward, A. S.: Empirical Evidence of Dynamic Hydrogeomorphic Feature Inundation in a Lowland Floodplain, Hydrological Processes, 39, e70043, https://doi.org/10.1002/hyp.70043, 2025.

Chen, X., Kumar, M., deB Richter, D., and Mau, Y.: Impact of gully incision on hillslope hydrology, Hydrological Processes, 34, 3848–3866, https://doi.org/10.1002/hyp.13845, 2020.

Clark, M. P., Rupp, D. E., Woods, R. A., Tromp-van Meerveld, H. J., Peters, N. E., and Freer, J. E.: Consistency between hydrological models and field observations: linking processes at the hillslope scale to hydrological responses at the watershed scale, Hydrological Processes, 23, 311–319, https://doi.org/10.1002/hyp.7154, 2009.

Collins, M. E., Doolittle, J. A., and Rourke, R. V.: Mapping Depth to Bedrock on a Glaciated Landscape with Ground-Penetrating Radar, Soil Science Society of America Journal, 53, 1806–1812, https://doi.org/10.2136/sssaj1989.03615995005300060032x, 1989.

Cook, T. A.: Stratigraphy and structure of the central Talladega slate belt, Alabama Appalachians, in: Tectonic Studies in the Talladega and Carolina Slate Belts, Southern Appalachian Orogen, edited by: Bearce, D. N., Black, W. W., Kish, S. A., and Tull, J. F., Geological Society of America, 0, https://doi.org/10.1130/SPE191-p47, 1982.

Costigan, K. H., Jaeger, K. L., Goss, C. W., Fritz, K. M., and Goebel, P. C.: Understanding controls on flow permanence in intermittent rivers to aid ecological research: integrating meteorology, geology and land cover, Ecohydrology, 9, 1141–1153, https://doi.org/10.1002/eco.1712, 2016.

Dralle, D. N., Karst, N. J., Charalampous, K., Veenstra, A., and Thompson, S. E.: Event-scale power law recession analysis: quantifying methodological uncertainty, Hydrology and Earth System Sciences, 21, 65–81, https://doi.org/10.5194/hess-21-65-2017, 2017.

Durighetto, N. and Botter, G.: On the Relation Between Active Network Length and Catchment Discharge, Geophysical Research Letters, 49, e2022GL099500, https://doi.org/10.1029/2022GL099500, 2022.

https://doi.org/10.5194/egusphere-2026-4201
Preprint. Discussion started: 27 July 2026

Feminella, J. W.: Comparison of Benthic Macroinvertebrate Assemblages in Small Streams along a Gradient of Flow Permanence, Journal of the North American Benthological Society, 15, 651–669, https://doi.org/10.2307/1467814, 1996.

Fryirs, K. A. and Brierley, G. J.: What's in a name? A naming convention for geomorphic river types using the River Styles Framework, PLOS ONE, 13, e0201909, https://doi.org/10.1371/journal.pone.0201909, 2018.

Godsey, S. E. and Kirchner, J. W.: Dynamic, discontinuous stream networks: hydrologically driven variations in active drainage density, flowing channels and stream order, Hydrological Processes, 28, 5791–5803, https://doi.org/10.1002/hyp.10310, 2014.

Griffith, G. E., Omernik, J. M., Comstock, J. A., Lawrence, S., Martin, G., Goddard, A., Hulcher, V. J., and Foster, T.: Ecoregions of Alabama, U.S. Environmental Protection Agency, National Health and Environmental Effects Research Laboratory, Corvallis, OR, 2001.

Harman, C. J., Sivapalan, M., and Kumar, P.: Power law catchment-scale recessions arising from heterogeneous linear small-scale dynamics, Water Resources Research, 45, https://doi.org/10.1029/2008WR007392, 2009.

Harvey, J. and Gooseff, M.: River corridor science: Hydrologic exchange and ecological consequences from bedforms to basins, Water Resources Research, 51, 6893–6922, https://doi.org/10.1002/2015WR017617, 2015.

Hester, E. T., McEwen, A. M., Kim, B.-J., and Rost, E. A.: Abundance, distribution, and geometry of naturally occurring streambank soil pipes, Freshwater Science, 39, 735–751, https://doi.org/10.1086/711655, 2020.

Holbrook, W. S., Riebe, C. S., Elwaseif, M., L. Hayes, J., Basler-Reeder, K., L. Harry, D., Malazian, A., Dosseto, A., C. Hartsough, P., and W. Hopmans, J.: Geophysical constraints on deep weathering and water storage potential in the Southern Sierra Critical Zone Observatory, Earth Surface Processes and Landforms, 39, 366–380, https://doi.org/10.1002/esp.3502, 2014.

Hrachowitz, M., Soulsby, C., Tetzlaff, D., Dawson, J. J. C., and Malcolm, I. A.: Regionalization of transit time estimates in montane catchments by integrating landscape controls, Water Resources Research, 45, https://doi.org/10.1029/2008WR007496, 2009.

Hynes, H. B. N.: The stream and its valley, SIL Proceedings, 1922-2010, 19, 1–15, https://doi.org/10.1080/03680770.1974.11896033, 1975.

Jachens, E. R., Roques, C., Rupp, D. E., and Selker, J. S.: Streamflow Recession Analysis Using Water Height, Water Resources Research, 56, e2020WR027091, https://doi.org/10.1029/2020WR027091, 2020.

https://doi.org/10.5194/egusphere-2026-4201
Preprint. Discussion started: 27 July 2026

Jencso, K. G. and McGlynn, B. L.: Hierarchical controls on runoff generation: Topographically driven hydrologic connectivity, geology, and vegetation, Water Resources Research, 47, https://doi.org/10.1029/2011WR010666, 2011.

Jencso, K. G., McGlynn, B. L., Gooseff, M. N., Wondzell, S. M., Bencala, K. E., and Marshall, L. A.: Hydrologic connectivity between landscapes and streams: Transferring reach- and plot-scale understanding to the catchment scale, Water Resources Research, 45, https://doi.org/10.1029/2008WR007225, 2009.

Jencso, K. G., McGlynn, B. L., Gooseff, M. N., Bencala, K. E., and Wondzell, S. M.: Hillslope hydrologic connectivity controls riparian groundwater turnover: Implications of catchment structure for riparian buffering and stream water sources, Water Resources Research, 46, https://doi.org/10.1029/2009WR008818, 2010.

Jones, C. N., Evenson, G. R., McLaughlin, D. L., Vanderhoof, M. K., Lang, M. W., McCarty, G. W., Golden, H. E., Lane, C. R., and Alexander, L. C.: Estimating restorable wetland water storage at landscape scales, Hydrological Processes, 32, 305–313, https://doi.org/10.1002/hyp.11405, 2018.

Jones, C. N., Nelson, N. G., and Smith, L. L.: Featured Collection Introduction: The Emerging Science of Aquatic System Connectivity I, JAWRA Journal of the American Water Resources Association, 55, 287–293, https://doi.org/10.1111/1752-1688.12739, 2019.

Kirker, A., Jones, C. N., Peterson, D. M., Tatariw, C., Nettles, J., and Chen, X.: Storage, Connectivity, and Stream Drying in Headwater Systems: Modeling Across Hydrogeomorphic Features, ESS Open Archive [preprint], https://doi.org/10.22541/essoar.175330904.43292818/v1, 2026.

Kopaska-Merkel, D. C., Dean, L. S., and Moore, J. D.: HYDROGEOLOGY AND VULNERABILITY TO CONTAMINATION OF MAJOR AQUIFERS IN ALABAMA: AREA 5, 2000.

Krakauer, N. Y. and Temimi, M.: Stream recession curves and storage variability in small watersheds, Hydrology and Earth System Sciences, 15, 2377–2389, https://doi.org/10.5194/hess-15-2377-2011, 2011.

Larkin, R. G. and Sharp, J. M., JR.: On the relationship between river-basin geomorphology, aquifer hydraulics, and ground-water flow direction in alluvial aquifers, GSA Bulletin, 104, 1608–1620, https://doi.org/10.1130/0016-7606(1992)104%253C1608:OTRBRB%253E2.3.CO;2, 1992.

Larned, S. T., Schmidt, J., Datry, T., Konrad, C. P., Dumas, J. K., and Diettrich, J. C.: Longitudinal river ecohydrology: flow variation down the lengths of alluvial rivers, Ecohydrology, 4, 532–548, https://doi.org/10.1002/eco.126, 2011.

Loheide, S. P. and Booth, E. G.: Effects of changing channel morphology on vegetation, groundwater, and soil moisture regimes in groundwater-dependent ecosystems, Geomorphology, 126, 364–376, https://doi.org/10.1016/j.geomorph.2010.04.016, 2011.

McDonnell, J. J., Sivapalan, M., Vaché, K., Dunn, S., Grant, G., Haggerty, R., Hinz, C., Hooper, R., Kirchner, J., Roderick, M. L., Selker, J., and Weiler, M.: Moving beyond heterogeneity and process complexity: A new vision for watershed hydrology, Water Resources Research, 43, https://doi.org/10.1029/2006WR005467, 2007.

McDonnell, J. J., Evaristo, J., Bladon, K. D., Buttle, J., Creed, I. F., Dymond, S. F., Grant, G., Iroume, A., Jackson, C. R., Jones, J. A., Maness, T., McGuire, K. J., Scott, D. F., Segura, C., Sidle, R. C., and Tague, C.: Water sustainability and watershed storage, Nat Sustain, 1, 378–379, https://doi.org/10.1038/s41893-018-0099-8, 2018.

McGlynn, B. L., McDonnell, J. J., Seibert, J., and Kendall, C.: Scale effects on headwater catchment runoff timing, flow sources, and groundwater-streamflow relations, Water Resources Research, 40, https://doi.org/10.1029/2003WR002494, 2004.

McGuire, K., McDonnell, J., Weiler, M., Kendall, C., McGlynn, B., Welker, J., and Seibert, J.: The role of topography on catchment-scale water residence time, Water Resources Research, 41, https://doi.org/10.1029/2004WR003657, 2005.

McLaughlin, D. L., Kaplan, D. A., and Cohen, M. J.: A significant nexus: Geographically isolated wetlands influence landscape hydrology, Water Resources Research, 50, 7153–7166, https://doi.org/10.1002/2013WR015002, 2014.

McNamara, J. P., Tetzlaff, D., Bishop, K., Soulsby, C., Seyfried, M., Peters, N. E., Aulenbach, B. T., and Hooper, R.: Storage as a Metric of Catchment Comparison, Hydrological Processes, 25, 3364–3371, https://doi.org/10.1002/hyp.8113, 2011.

Menichino, G. T. and Hester, E. T.: The effect of macropores on bi-directional hydrologic exchange between a stream channel and riparian groundwater, Journal of Hydrology, 529, 830–842, https://doi.org/10.1016/j.jhydrol.2015.09.005, 2015.

Montgomery, D. R. and Buffington, J. M.: Channel processes, classification, and response, River ecology and management, 112, 1250–1263, 1998.

Newcomb, S. K. and Godsey, S. E.: Nonlinear Riparian Interactions Drive Changes in Headwater Streamflow, Water Resources Research, 59, e2023WR034870, https://doi.org/10.1029/2023WR034870, 2023.

NOAA National Centers for Environmental information: Climate at a Glance: County Time Series, 2025.

Onda, Y., Komatsu, Y., Tsujimura, M., and Fujihara, J.: The role of subsurface runoff through bedrock on storm flow generation, Hydrological Processes, 15, 1693–1706, https://doi.org/10.1002/hyp.234, 2001.

Peters, N. E. and Aulenbach, B. T.: Water storage at the Panola Mountain Research Watershed, Georgia, USA, Hydrological Processes, 25, 3878–3889, https://doi.org/10.1002/hyp.8334, 2011.

Peterson, D. M., Jones, C. N., Plattner, A. M., Shogren, A. J., and Godsey, S. E.: Using Hydrogeomorphic Features to Quantify Structural and Functional Hydrologic Connectivity in a Coastal Plain Headwater Stream, Water Resources Research, 61, e2024WR038533, https://doi.org/10.1029/2024WR038533, 2025.

Peterson, D. M., Jones, C. N., Zarek, K., Wolford, M., Smith, C., Bond, C. T., Plont, S., Kraft, M., Speir, S., Zipper, S., Godsey, S. E., Benstead, J., Shogren, A., Kuehn, K., and Atkinson, C.: Using Physiography as a Lens to Understand Stream Network Expansion and Contraction Across Spatiotemporal Scales, EarthArXiv [preprint], https://eartharxiv.org/repository/view/9484/, 2026.

Pfister, L., Martínez-Carreras, N., Hissler, C., Klaus, J., Carrer, G. E., Stewart, M. K., and McDonnell, J. J.: Bedrock geology controls on catchment storage, mixing, and release: A comparative analysis of 16 nested catchments, Hydrological Processes, 31, 1828–1845, https://doi.org/10.1002/hyp.11134, 2017.

Plont, S., Peterson, D. M., Smith, C. R., Bond, C. T., Tchamba, A. L. K., Wolford, M. A., Zarek, K., Speir, S. L., Jones, C. N., Benstead, J. P., Busch, M. H., Hale, R. L., Brown, C. L., Seybold, E. C., Shogren, A. J., Kuehn, K. A., You, Y., Jackson, C. R., Burgin, A. J., and Atkinson, C. L.: Hydrologic, biogeochemical, microbial, and macroinvertebrate responses to network expansion, contraction, and disconnection across headwater stream networks with distinct physiography in Alabama, USA, Earth System Science Data Discussions, 1–40, https://doi.org/10.5194/essd-2025-559, 2025.

Ploum, S. W., Leach, J. A., Laudon, H., and Kuglerová, L.: Groundwater, Soil, and Vegetation Interactions at Discrete Riparian Inflow Points (DRIPs) and Implications for Boreal Streams, Front. Water, 3, https://doi.org/10.3389/frwa.2021.669007, 2021.

Ponta, G.: Geologic Framework of Karst Aquifer Systems in Alabama, Sinkhole Conference 2018, 2018.

Prancevic, J. P. and Kirchner, J. W.: Topographic Controls on the Extension and Retraction of Flowing Streams, Geophysical Research Letters, 46, 2084–2092, https://doi.org/10.1029/2018GL081799, 2019.

Price, K.: Effects of watershed topography, soils, land use, and climate on baseflow hydrology in humid regions: A review, Progress in Physical Geography: Earth and Environment, 35, 465–492, https://doi.org/10.1177/0309133311402714, 2011.

https://doi.org/10.5194/egusphere-2026-4201
Preprint. Discussion started: 27 July 2026

Pringle, C. M.: Hydrologic Connectivity and the Management of Biological Reserves: A Global Perspective, Ecological Applications, 11, 981–998, https://doi.org/10.1890/1051-0761(2001)011%255B0981:HCATMO%255D2.0.CO;2, 2001.

R Core Team: R: A Language and Environment for Statistical Computing, 2024.

Rosgen, D. L.: A classification of natural rivers, CATENA, 22, 169–199, https://doi.org/10.1016/0341-8162(94)90001-9, 1994.

Sayama, T., McDonnell, J. J., Dhakal, A., and Sullivan, K.: How much water can a watershed store?, Hydrological Processes, 25, 3899–3908, https://doi.org/10.1002/hyp.8288, 2011.

Shaw, S. B. and Riha, S. J.: Examining individual recession events instead of a data cloud: Using a modified interpretation of dQ/dt–Q streamflow recession in glaciated watersheds to better inform models of low flow, Journal of Hydrology, 434–435, 46–54, https://doi.org/10.1016/j.jhydrol.2012.02.034, 2012.

Soil Survey Staff, Natural Resources Conservation Service, United States Department of Agriculture: Web Soil Survey, n.d.

Spence, C.: A Paradigm Shift in Hydrology: Storage Thresholds Across Scales Influence Catchment Runoff Generation, Geography Compass, 4, 819–833, https://doi.org/10.1111/j.1749-8198.2010.00341.x, 2010.

Squillace, P. J.: Observed and Simulated Movement of Bank-Storage Water, Groundwater, 34, 121–134, https://doi.org/10.1111/j.1745-6584.1996.tb01872.x, 1996.

Swenson, G. A.: Soil Survey of Jackson County, Alabama, U.S. Department of Agriculture, Soil Conservation Service, 238 pp., 1954.

Szabo, E. W., Osborne, W. E., Copeland, C. W., and Neathery, T. L.: Geologic map of Alabama, Geological Survey of Alabama, 1988.

Tashie, A., Scaife, C. I., and Band, L. E.: Transpiration and subsurface controls of streamflow recession characteristics, Hydrological Processes, 33, 2561–2575, https://doi.org/10.1002/hyp.13530, 2019.

Tashie, A., Pavelsky, T., and Band, L. E.: An Empirical Reevaluation of Streamflow Recession Analysis at the Continental Scale, Water Resources Research, 56, e2019WR025448, https://doi.org/10.1029/2019WR025448, 2020.

https://doi.org/10.5194/egusphere-2026-4201
Preprint. Discussion started: 27 July 2026

Tetzlaff, D., Birkel, C., Dick, J., Geris, J., and Soulsby, C.: Storage dynamics in hydropedological units control hillslope connectivity, runoff generation, and the evolution of catchment transit time distributions, Water Resources Research, 50, 969–985, https://doi.org/10.1002/2013WR014147, 2014.

Tromp-van Meerveld, H. J. and McDonnell, J. J.: Threshold relations in subsurface stormflow: 1. A 147-storm analysis of the Panola hillslope, Water Resources Research, 42, https://doi.org/10.1029/2004WR003778, 2006a.

Tromp-van Meerveld, H. J. and McDonnell, J. J.: Threshold relations in subsurface stormflow: 2. The fill and spill hypothesis, Water Resources Research, 42, https://doi.org/10.1029/2004WR003800, 2006b.

Turner, I. P., Brantley, E. F., and Shaw, J. N.: Floristic Composition of Alabama Piedmont Floodplains across a Gradient of Stream Channel Incision, amid, 174, 238–253, https://doi.org/10.1674/0003-0031-174.2.238, 2015.

Van Meter, K., Thompson, S. E., and Basu, N. B.: Chapter 11 - Human Impacts on Stream Hydrology and Water Quality, in: Stream Ecosystems in a Changing Environment, edited by: Jones, J. B. and Stanley, E. H., Academic Press, Boston, 441–490, https://doi.org/10.1016/B978-0-12-405890-3.00011-7, 2016.

Vietz, G. J., Rutherfurd, I. D., Fletcher, T. D., and Walsh, C. J.: Thinking outside the channel: Challenges and opportunities for protection and restoration of stream morphology in urbanizing catchments, Landscape and Urban Planning, 145, 34–44, https://doi.org/10.1016/j.landurbplan.2015.09.004, 2016.

Vogel, R. M. and Kroll, C. N.: Regional geohydrologic-geomorphic relationships for the estimation of low-flow statistics, Water Resources Research, 28, 2451–2458, https://doi.org/10.1029/92WR01007, 1992.

Ward, A. S., Schmadel, N. M., and Wondzell, S. M.: Simulation of dynamic expansion, contraction, and connectivity in a mountain stream network, Advances in Water Resources, 114, 64–82, https://doi.org/10.1016/j.advwatres.2018.01.018, 2018.

Wegener, P., Covino, T., and Wohl, E.: Beaver-mediated lateral hydrologic connectivity, fluvial carbon and nutrient flux, and aquatic ecosystem metabolism, Water Resources Research, 53, 4606–4623, https://doi.org/10.1002/2016WR019790, 2017.

Zarek, K., Jones, C. N., Peterson, D. M., Plont, S., Shogren, A. J., Tatariw, C., Speir, S. L., Mortazavi, B., and Burgin, A. J.: Investigating Spatial and Temporal Nitrogen Dynamics in a Forested Headwater Stream Over the Course of an Annual Drying Event, Journal of Geophysical Research: Biogeosciences, 130, e2024JG008522, https://doi.org/10.1029/2024JG008522, 2025.

https://doi.org/10.5194/egusphere-2026-4201
Preprint. Discussion started: 27 July 2026

Zecharias, Y. B. and Brutsaert, W.: Recession characteristics of groundwater outflow and base flow from mountainous watersheds, Water Resources Research, 24, 1651–1658, https://doi.org/10.1029/WR024i010p01651, 1988.

Zimmer, M. A. and McGlynn, B. L.: Lateral, Vertical, and Longitudinal Source Area Connectivity Drive Runoff and Carbon Export Across Watershed Scales, Water Resources Research, 54, 1576–1598, https://doi.org/10.1002/2017WR021718, 2018.

Zipper, S. C., Hammond, J. C., Shanafield, M., Zimmer, M., Datry, T., Jones, C. N., Kaiser, K. E., Godsey, S. E., Burrows, R. M., Blaszczak, J. R., Busch, M. H., Price, A. N., Boersma, K. S., Ward, A. S., Costigan, K., Allen, G. H., Krabbenhoft, C. A., Dodds, W. K., Mims, M. C., Olden, J. D., Kampf, S. K., Burgin, A. J., and Allen, D. C.: Pervasive changes in stream intermittency across the United States, Environ. Res. Lett., 16, 084033, https://doi.org/10.1088/1748-9326/ac14ec, 2021.

Zuecco, G., Penna, D., Borga, M., and van Meerveld, H. J.: A versatile index to characterize hysteresis between hydrological variables at the runoff event timescale, Hydrological Processes, 30, 1449–1466, https://doi.org/10.1002/hyp.10681, 2016.